



Publication Year	2012
Acceptance in OA @INAF	2023-02-20T14:24:18Z
Title	Planck/LFI: DPC Processing and Use of Pointing Information
Authors	MARIS, Michele; GALEOTTA, Samuele; SANDRI, MAURA; VILLA, Fabrizio; FRAILIS, Marco; et al.
Handle	http://hdl.handle.net/20.500.12386/33606
Number	PL-LFI-OAT-TN-087



INAF/OATs
LFI Project System Team

Planck LFI

TITLE: **Planck/LFI: DPC Processing and Use of Pointing Information**

DOC. TYPE: Technical Note

PROJECT REF.: PL-LFI-OAT-TN-087

ISSUE/REV.: 0.7.b

PAGE: 1 of 37

DATE: March 30, 2012

Prepared by	M.Marisi, S.Galeotta, M.Sandri, F.Villa, M.Frailis, A.Zacchei	March 30, 2012
Agreed by	M. Bersanelli LFI Instrument Scientist A. Zacchei LFI/DPC manager C.R. Butler LFI Program Manager	
Approved by	N. Mandolesi LFI Principal Investigator	



CHANGE RECORD

Issue	Date	Sheet	Description of change	Release
0.0	Feb 10, 2012	All	First draft of document, titled: "Rotating Beam on the Sky"	0.0
0.4	Feb 24, 2012	All	First draft of document	0.4
0.5	Mar 6, 2012	All	Final number assigned. Reference direction now is South.	0.5
0.5b	Mar 7, 2012	All	Added validation on the real case	0.7b
0.6	Mar 8, 2012	All	Typos corrections, added figures of reference frames	0.6
0.7	Mar 16, 2012	All	Improved definition of ax2det matrix	0.7
0.7.a	Mar 26, 2012	All	Verified the definition of the ax2det matrix against GRASP 9 and old ESTEC document, an appendix added, documentation updated.	0.7.a
0.7.b	Mar 30, 2012	All	Added definition and coordinate transforms between beam reference frame and UV plane	0.7.b



DISTRIBUTION LIST

Recipient	Company/Institute	E-mail address	Sent
Michele Maris	INAF/OATS	maris@oats.inaf.it	March 30, 2012
Samuele Galeotta	INAF/OATS	galeotta@oats.inaf.it	March 30, 2012
Andrea Zacchei	INAF/OATS	zacchei@oats.inaf.it	March 30, 2012
Marco Frailis	INAF/OATS	frailis@oats.inaf.it	March 30, 2012



Contents

1	Applicable and Reference Documents	1
2	Scope of the document	2
2.1	Limits of Applicability	2
3	Introduction	2
3.1	The <code>detpoint_pol</code> object	2
3.2	Definition of the Beam Attitude Matrix	3
3.3	Definition of ψ	3
4	Definition of a Validation Case	4
4.1	Describing a Scan Circle	4
4.2	Spin axis on the ecliptic, Polarization S axis aligned with $\hat{\mathbf{X}}_{\text{los}}$	8
4.3	Spin axis on the ecliptic, Polarization S axis tilted with respect to $\hat{\mathbf{X}}_{\text{los}}$	9
4.4	Spin axis tilted on the ecliptic, Polarization S axis aligned with $\hat{\mathbf{X}}_{\text{los}}$	10
4.5	ClockWise v.z. AntiClockWise	15
5	Extracting beam attitude	16
5.1	Build the <code>ax2det</code> matrix	16
5.2	Form the Attitude Conversion Matrix from Quaternions	17
5.3	Form rotation matrices for astrometric colatitude and longitude	17
5.4	Extract <code>psi</code>	18
6	Usage of the angles: draw the polarization axis S and M	19
6.1	Step 1: form pointing matrices	19
6.2	Step 2: form local polarization matrices	19
6.3	Step 3: form beam to ecliptical matrices	19
7	Rotating a GRASP map	21
7.1	Total Power	21
7.2	Polarization	21
8	Converting between UV plane and polar coordinates	22
9	Validating a Real Case	23
9.1	Selecting pointing period and samples	23
9.2	Selecting the feed-horns	23
9.3	Validating feed-horn 24	23
9.4	Validating feed-horn 25	26
A	Reference Frames	28
A.1	IAU Astrometric Ecliptical Reference Frame	28
A.2	COSMO Ecliptical Reference Frame	28
A.3	Spin Axis Reference Frame	29
A.4	SpaceCraft Reference Frame	29
A.5	Telescope Reference Frame (also LOS RF)	29
A.6	Beam Reference Frame	30
B	Two examples of validation of the <code>ax2det</code> matrix	31



C Calculations and tables for the first validation example	31
D Tables	34



LIST OF ABBREVIATIONS

acronym	Explanation
DMC	Data Management Component
FPdb	Focal Plane database
LFI	Low Frequency Instrument
HFI	High Frequency Instrument
IT	Information Technology
LOS	Line-of-Sight
RF	Reference Frame
PoV	Point of View
SSB	Solar System Baricenter
SSO	Solar System Object
TBC	To Be Confirmed
TBD	To Be Defined
TOD	Time Ordered Data
TODs	Plural of TOD
TOI	Time Ordered Information
TODs	Plural of TOI



1 Applicable and Reference Documents

Applicable Documents

- [AD-1] Unknown Author, 2009 *Planck/LFI DPC: LFI RIMO* Planck/LFI Int.Rep.: PL-LFI-OAT-TN-unknown, Issue 8.1, December 2009
- [AD-2] Pablo Fosalba¹, Arturo Martín Polegre² *Conventions and Coordinate Systems for the Polarized Radiation Patterns Simulated at ESTEC using GRASP8* Unnumbered document ESTEC, November 22, 2000

Reference Documents

- [RD-1] Unknown Author, 2000 *Planck Telescope Design Specification* Internal Report ESTEC/SCI-PT-RS-07024, 31 August 2000
- [RD-2] M. Sandri, F. Villa *Planck/LFI: Main Beam Locations and Polarization Alignment for the LFI Baseline FPU* PL-LFI-PST-TN-027 July, 2001
- [RD-3] M. Sandri *Bandwidth dependence of LFI main beams* PL-LFI-PST-TN-075 October 23, 2006
- [RD-4] M. Sandri, F. Villa *LFI Main Beams at 30 GHz* PL-LFI-PST-TN-040 February 22, 2005
- [RD-5] M. Sandri *LFI Beams Delivery Format Specifications* PL-LFI-PST-TN-044 July 15, 2003
- [RD-6] M. Sandri, F. Villa *LFI Main Beams at 44 GHz* PL-LFI-PST-TN-061 February 22, 2005
- [RD-7] M. Sandri, F. Villa *LFI Main Beams at 70 GHz* PL-LFI-PST-TN-062 February 22, 2005



2 Scope of the document

Beam attitude is the combination of beam pointing (where the beam is looking in the sky) and beam orientation (how the beam is oriented in the sky) and it is the combination of pointing and orientation information.

Scope of this document is to describe how the pointing information is processed the LFI/DPC pipeline to derive the beam attitude information. The document also is motivated by the need to fix a reference cases for validation.

There is a number of operations which must be documented

1. Define a case for validation of beam attitude information recovery and use;
2. Derive beam attitude information from the spacecraft attitude information and the focal plane database
3. Use beam attitude information to properly place in the sky a beam with S or M polarization properly oriented.
4. Use beam attitude information to properly place in the sky a map of the beam properly oriented.
5. Use beam attitude information to place in the sky an elliptical beam properly oriented.

2.1 Limits of Applicability

The document refers to definitions, procedures and operations, in use at the PLANCK/LFI DPC. Other departments in the PLANCK collaboration can use different definitions and procedures.

3 Introduction

Beam attitude is the combination of beam pointing (where the beam is looking in the sky) and beam orientation (how the beam is oriented in the sky) and it is the combination of pointing and orientation information. In particular beam attitude shall return the orientation of all of the axis of the beam reference frame in order to allow proper orientation of polarization components, main beam and sidelobes.

3.1 The `detpoint_pol` object

The DPC provides for each radiometer and sampling time an object `detpoint_pol` which is represented by a tuple of the kind

$$(OBT, SCET, phi, theta, psi) \quad (1)$$

where

<code>OBT</code>	t_{obt}	OBT of the sample
<code>SCET</code>	t_{scet}	SCET of the sample
<code>phi</code>	ϕ	Pointing Longitude of the beam in the Ecliptical Reference Frame
<code>theta</code>	θ	Pointing Colatitude of the beam in the Ecliptical Reference Frame
<code>psi</code>	ψ	Orientation of Polarization S axis $\hat{\mathbf{I}}_S$ in the Ecliptical Reference Frame (see Sect. 3.3)



In the following the distinction between t_{obt} and t_{scet} will be omitted, unless necessary, and time t will be used in place. The content tuple (1) is the only piece of time-dependent information that an end user accesses in order to properly compute the beam attitude in the ecliptical reference frame.

3.2 Definition of the Beam Attitude Matrix

The matrix describing the transformation from the beam reference frame (see Appendix A.6) to the ecliptic reference frame (see Appendix A.1) is the product of three rotations: $\mathbf{R}_\phi \mathbf{R}_\theta \mathbf{R}_z(\psi)$ whose form will be described later. Assuming to be in the beam reference frame, and to denote with $\hat{\mathbf{P}} = \hat{\mathbf{e}}_z$ axis the pointing direction, with $\hat{\mathbf{\Pi}}_S = \hat{\mathbf{e}}_x$ the S axis polarization direction and $\hat{\mathbf{e}}_y = \hat{\mathbf{P}} \times \hat{\mathbf{\Pi}}_S$, the user can derive the axis describing the beam, its pointing and its orientation in the ecliptic reference frame as

$$\begin{aligned}\hat{\mathbf{P}}_{\text{Ecl}} &= \mathbf{R}_\phi \mathbf{R}_\theta \mathbf{R}_z(\psi) \hat{\mathbf{e}}_z; \\ \hat{\mathbf{\Pi}}_S^{\text{Ecl}} &= \mathbf{R}_\phi \mathbf{R}_\theta \mathbf{R}_z(\psi) \hat{\mathbf{e}}_x; \\ \hat{\mathbf{\Pi}}_M^{\text{Ecl}} &= \mathbf{R}_\phi \mathbf{R}_\theta \mathbf{R}_z(\psi + \psi_{\text{pol}}) \hat{\mathbf{e}}_x. \\ \hat{\mathbf{B}}_a^{\text{Ecl}} &= \mathbf{R}_\phi \mathbf{R}_\theta \mathbf{R}_z(\psi + \psi_{\text{ell}}) \hat{\mathbf{e}}_x.\end{aligned}\tag{2}$$

where $\hat{\mathbf{P}}_{\text{Ecl}}$ is the pointing vector in the ecliptic, $\hat{\mathbf{\Pi}}_S^{\text{Ecl}}$ the already mentioned polarization S axis, $\hat{\mathbf{\Pi}}_M^{\text{Ecl}}$ the polarization M axis, and $\hat{\mathbf{B}}_a^{\text{Ecl}}$ the major axis of the main beam in the elliptical gaussian approximation. The axis $\hat{\mathbf{\Pi}}_S^{\text{Ecl}}$, $\hat{\mathbf{\Pi}}_M^{\text{Ecl}}$ and $\hat{\mathbf{B}}_a^{\text{Ecl}}$ are coplanar and normal to $\hat{\mathbf{P}}_{\text{Ecl}}$. They are defined in the plane tangent to the ecliptical sphere in the point pointing direction $\hat{\mathbf{P}}_{\text{Ecl}}$. The angles ψ_{pol} and ψ_{ell} are measured in the tangent plane seen from outside the sphere ($\hat{\mathbf{P}}_{\text{Ecl}}$ comes out from the plane) anticlockwise (clockwise if their values are negative).

3.3 Definition of ψ

The same convention of an anticlockwise positive (clockwise negative) is assumed for ψ which is the angle between $\hat{\mathbf{\Pi}}_S$ and the direction of the South pole, $\hat{\mathcal{S}}$, in tangent plane (see Fig. 2).



4 Definition of a Validation Case

Before describing the DPC algorithm it is worth to define a set of validation cases. Validation is obtained by comparing the output of the procedure against a set of well constrained cases which can be easily computed building a chain of cases of increasing level of complexity. So that

Section 4.1 is the scan circle model used here.

Section 4.2 refers to a scan circle with Spin axis on the ecliptic plane, at zero ecliptical longitude and latitude, with the beam in the LOS and $\hat{\mathbf{I}}_S$ aligned with $\hat{\mathbf{X}}_{\text{los}}$.

Section 4.3 allows the beam to be reoriented with respect to the LOS.

Section 4.4 allows the spin axis to be tilted with respect to the ecliptic plane. In particular the qualitative behaviour of ψ depends on the critical values $|b_{\text{spin}}| = 90^\circ - \beta$. Infact for $|b_{\text{spin}}| < 90^\circ - \beta$. the scan circle does not include either the North or the South ecliptical poles while outside those limits it does it.

4.1 Describing a Scan Circle

In our case the strategy is that to start with a minimal model in which the spin axis $\hat{\mathbf{S}}$ has a constant position in the ecliptical reference frame. The telescope LOS, $\hat{\mathbf{P}}_{\text{LOS}}$, scans the sky at a constant rate drawing a circle of fixed half aperture $\beta = \arccos \hat{\mathbf{P}}_{\text{LOS}} \cdot \hat{\mathbf{S}}$. The circle is scanned anticlockwise when the spin axis is seen coming out from the sphere, so that $\phi_{\text{los}} = 0^\circ$ occurs when the LOS colatitude $\Theta_{\text{los}} = \arccos \hat{\mathbf{P}}_{\text{LOS}} \cdot \hat{\mathbf{S}}$ has its minimnal value. In order to describe this rotation a convenient reference frame is the Spin Reference Frame (see Appendix A.3 and Fig. 1) defined as the reference frame having

- $\hat{\mathbf{X}}_{\text{spin}}$ the X axis: the spin axis;
- $\hat{\mathbf{Z}}_{\text{spin}}$ the Z axis: an axis normal to $\hat{\mathbf{X}}_{\text{spin}}$ in the plane defined by the ecliptical Z axis and $\hat{\mathbf{X}}_{\text{spin}}$;
- $\hat{\mathbf{Y}}_{\text{spin}}$ the Y axis: given by the usual $\hat{\mathbf{Z}}_{\text{spin}} \times \hat{\mathbf{X}}_{\text{spin}}$.

for a fixed spin axis this reference frame is fixed in the sky. In this frame

$$\hat{\mathbf{P}}_{\text{LOS}} = \begin{pmatrix} 1 & 0 & 0 \\ 0 & \cos \phi_{\text{los}} & -\sin \phi_{\text{los}} \\ 0 & \sin \phi_{\text{los}} & \cos \phi_{\text{los}} \end{pmatrix} \begin{pmatrix} \cos \beta \\ 0 \\ \sin \beta \end{pmatrix} \quad (3)$$

Feed-horns are located in the vicinity of LOS in order to transfer the LOS coordinates to Feed-horns coordinates the it is sufficient to consider the LOS reference frame defined as

- $\hat{\mathbf{Z}}_{\text{los}}$ the Z axis: Telescope LOS at an angle β from the spin axis;
- $\hat{\mathbf{X}}_{\text{los}}$ the X axis: an axis normal to Z oriented toward the spin axis;
- $\hat{\mathbf{Y}}_{\text{los}}$ the Y axis: given by the usual $\hat{\mathbf{Z}}_{\text{los}} \times \hat{\mathbf{Y}}_{\text{los}}$.

So each feed-horn scans the sky in the same manner as the LOS but with some slightly wider or narrower boresight angle β_{th} and a different phase $\varphi_{\hat{P}}$ slightly anticipating or delaying the LOS, and with $\varphi_{\hat{P}} = 0^\circ$ when $\hat{\mathbf{P}}_{\text{Ecl}}$ is at its minimal distance from the North Ecliptic Pole \mathcal{N} . The location and orientation of a beam in the LOS reference frame are encoded by three parameters in the optical database ϕ_{uv} , θ_{uv} and ψ_{uv} . The corresponding transforming matrix $\mathbf{U}_{\text{det}}^{\text{ax}}(\phi_{\text{uv}}, \theta_{\text{uv}}, \psi_{\text{uv}})$ reduces to identity matrix when $\phi_{\text{uv}} = 0^\circ$, $\theta_{\text{uv}} = 0^\circ$ and $\psi_{\text{uv}} = 0^\circ$. In this case the beam is located in the LOS and its polarization S axis, $\hat{\mathbf{I}}_S$ is oriented as X in the LOS reference frame. In this case the ψ angle can be derived from geometrical principles without to involve any rotation matrix or convention.

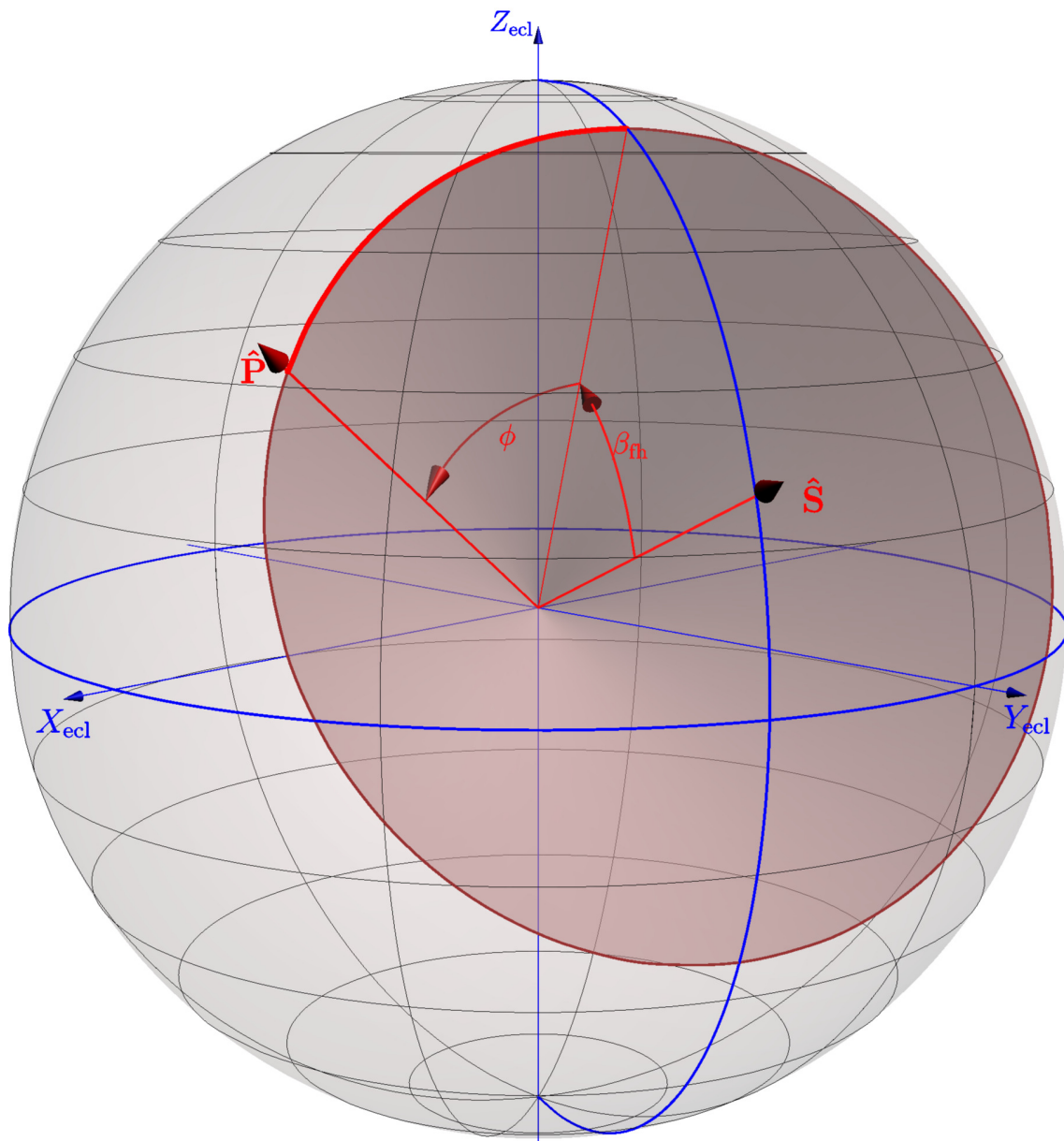


Figure 1: The Ecliptical Reference Frame (blue elements) and the Spin Axis Reference Frame (red elements). The cone represents the set of directions scanned by a scan circle with fixed spin axis. For graphical reasons the β_{fh} angle is smaller than that of any Feed-Horn in PLANCK and the tilt of the spin axis is much larger than any possible tilt in the scanning strategy.

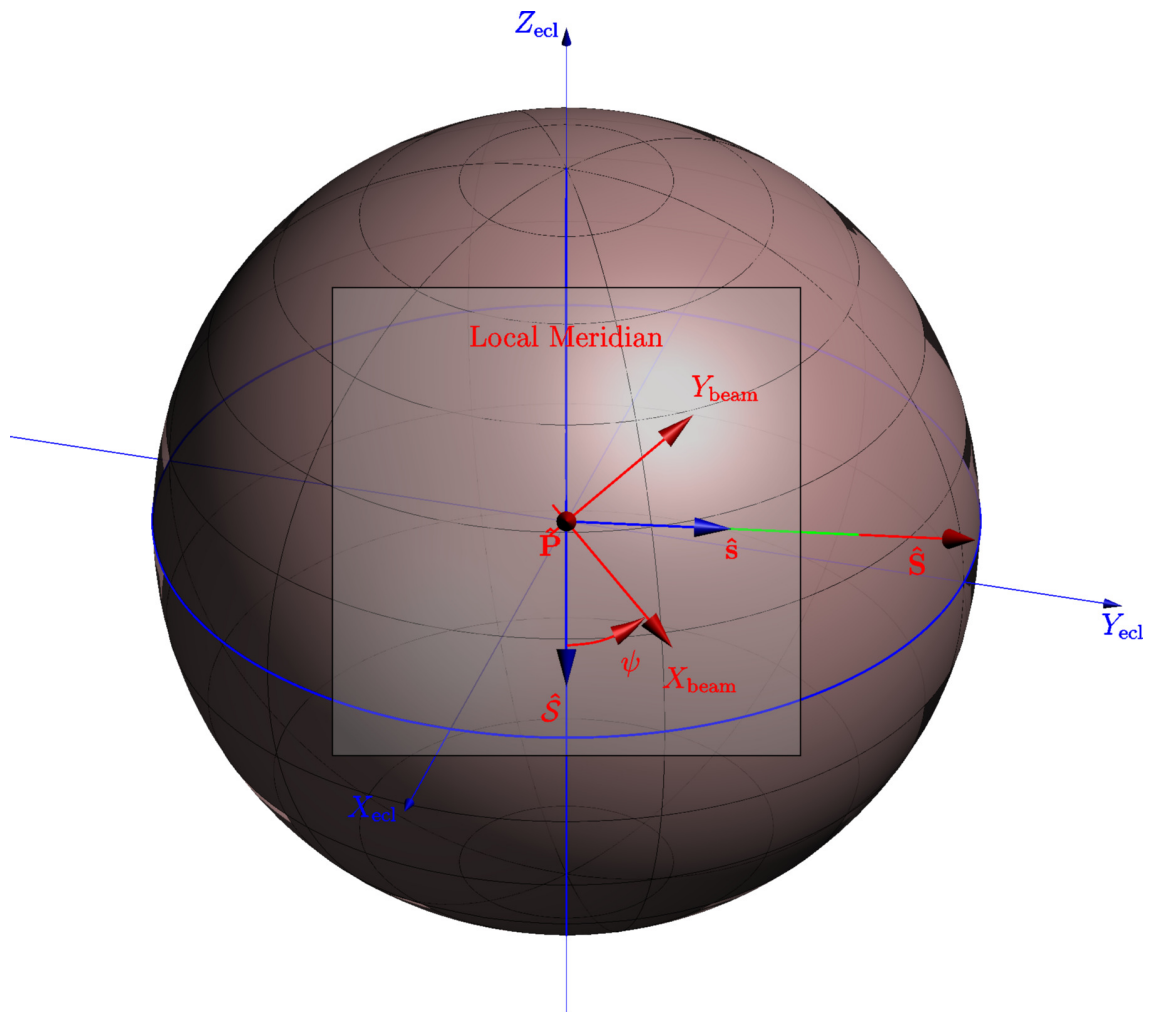


Figure 2: The Tangent Reference Frame (blue) and the Beam Reference Frame (red). The view is for an observer looking from the top of the pointing direction. The figure defines also the ψ angle.

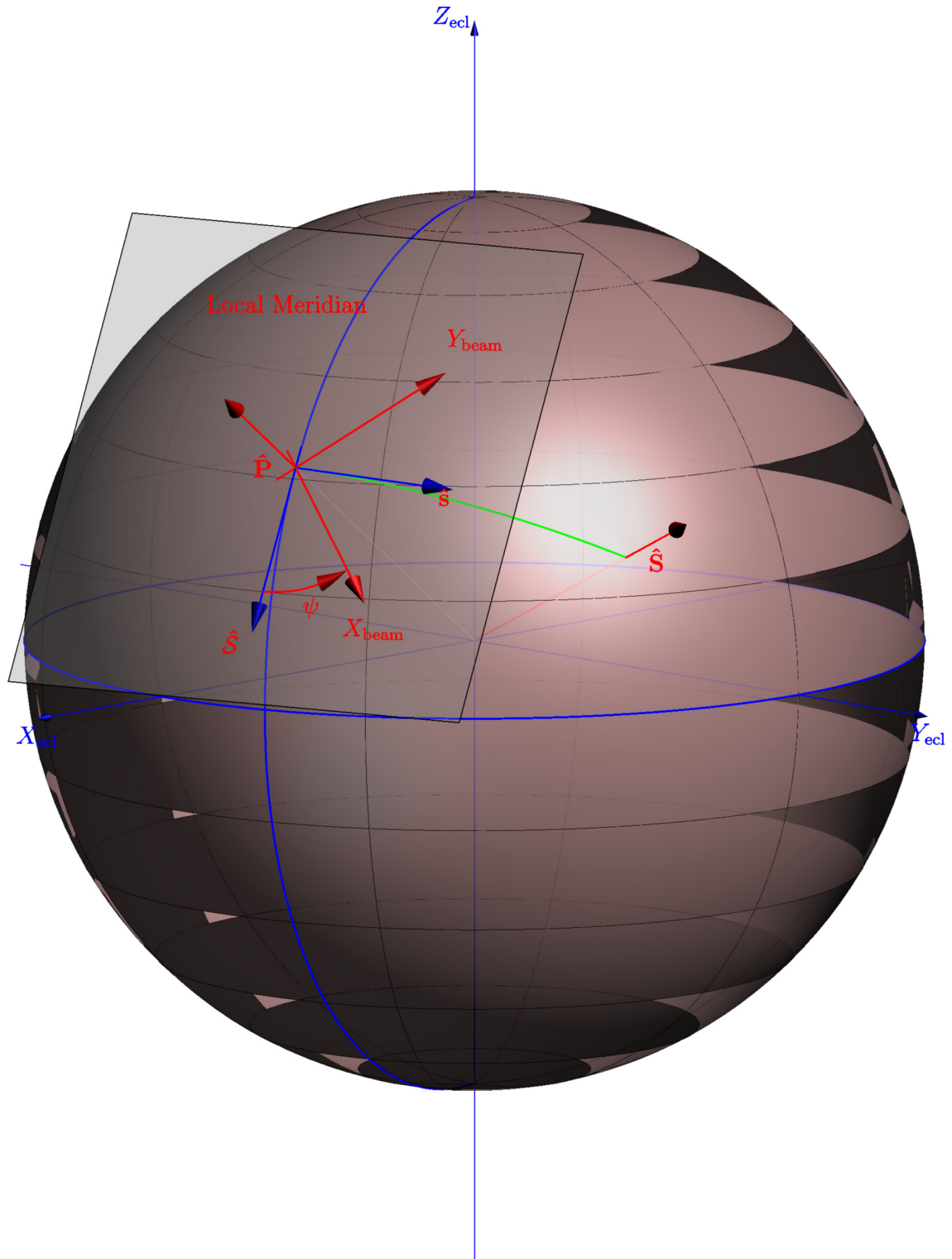


Figure 3: The same of Fig. 2 but with a different view.



4.2 Spin axis on the ecliptic, Polarization S axis aligned with $\hat{\mathbf{X}}_{\text{los}}$

We assume $\hat{\mathbf{S}} = \hat{\mathbf{X}}_{\text{ecl}} = (1, 0, 0)$. The beam is centered on the LOS and aligned along the X axis, so that in this case $\phi_{\text{uv}} = 0^\circ$, $\theta_{\text{uv}} = 0^\circ$ and $\psi_{\text{uv}} = 0^\circ$. In this way the angle expressing the orientation of $\hat{\mathbf{\Pi}}_{\text{S}}$ with respect to the local direction of the South Pole $\hat{\mathbf{S}}$ along the local meridian in the plane tangent to the celestial sphere defined by $\hat{\mathbf{P}}_{\text{Ecl}}$ is

$$\begin{aligned}\cos \psi_{\text{pol,S}} &= \hat{\mathbf{S}} \cdot \hat{\mathbf{s}} \\ \sin \psi_{\text{pol,S}} &= (\hat{\mathbf{S}} \times \hat{\mathbf{s}}) \cdot \hat{\mathbf{P}} \\ \psi_{\text{pol,S}} &= \arctan2(\sin \psi_{\text{pol,S}}, \cos \psi_{\text{pol,S}})\end{aligned}\quad (4)$$

The $\hat{\mathbf{s}}$ versor is the direction of the spin axis in the plane tangent to the celestial sphere, is the analogous of the $\hat{\mathbf{S}}$ versor, but taking the spin axis as the pole of the reference system. Of course in the LOS reference frame $\hat{\mathbf{s}} = \hat{\mathbf{X}}_{\text{los}}$. Both $\hat{\mathbf{S}}$ and $\hat{\mathbf{s}}$ versors at the $\hat{\mathbf{P}}$ location on the sphere can be derived from the $\hat{\mathbf{P}}$ definition

$$\begin{aligned}\hat{\mathbf{S}} &= \frac{\partial \hat{\mathbf{P}}}{\partial \theta} \\ \hat{\mathbf{s}} &= -\frac{\partial \hat{\mathbf{P}}}{\partial \beta} \\ \hat{\mathbf{Y}}_{\text{los}} &= \hat{\mathbf{P}} \times \hat{\mathbf{s}}\end{aligned}\quad (5)$$

the last definition comes from $\hat{\mathbf{s}} \equiv \hat{\mathbf{X}}_{\text{los}}$, and of course $\hat{\mathbf{P}} \cdot \hat{\mathbf{S}} = 0$ and $\hat{\mathbf{s}} \cdot \hat{\mathbf{P}} = 0$. Then having $\hat{\mathbf{P}}(\varphi_{\hat{\mathbf{P}}})$ to start from South and moving anticlockwise around $\hat{\mathbf{S}}$ increasing $\varphi_{\hat{\mathbf{P}}}$

$$\begin{aligned}\hat{\mathbf{P}} &= \begin{pmatrix} \cos \beta \\ -\sin \beta \sin \varphi_{\hat{\mathbf{P}}} \\ \sin \beta \cos \varphi_{\hat{\mathbf{P}}} \end{pmatrix} = \begin{pmatrix} \sin \theta \cos \phi \\ \sin \theta \sin \phi \\ \cos \theta \end{pmatrix}; \\ \hat{\mathbf{S}} &= \begin{pmatrix} \cos \theta \cos \phi \\ \cos \theta \sin \phi \\ -\sin \theta \end{pmatrix}; \\ \hat{\mathbf{s}} &= \begin{pmatrix} \sin \beta \\ \cos \beta \sin \varphi_{\hat{\mathbf{P}}} \\ -\cos \beta \cos \varphi_{\hat{\mathbf{P}}} \end{pmatrix}.\end{aligned}\quad (6)$$

For $\psi_{\text{uv}} = 0^\circ$ there are a number of subcases varying $\varphi_{\hat{\mathbf{P}}}$ tabulated in Tab. 3 in the appendix D, and plotted in Fig. 4 at intermediate angles, but the most significant are listed below while in Appendix C calculations are detailed

$\varphi_{\hat{\mathbf{P}}}$	ψ
0°	0°
45°	85.018931°
90°	90°
135°	94.98107°
180°	180°
225°	-94.98107°
270°	-90°
315°	-85.018931°

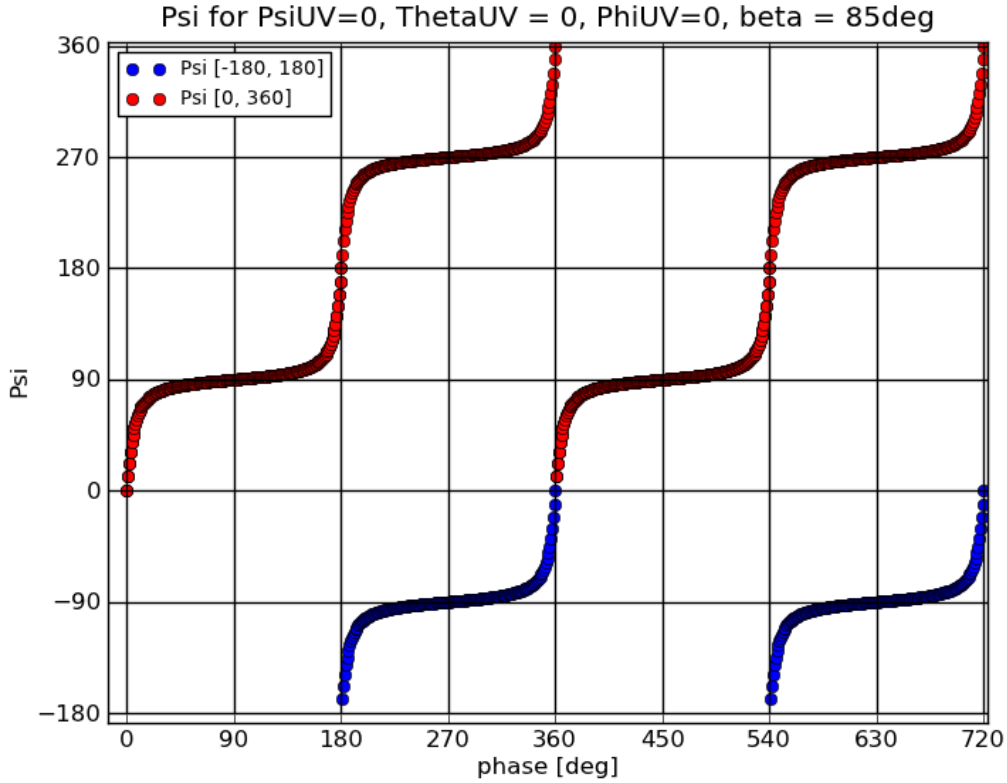


Figure 4: Values of ψ for $\beta = 85^\circ$ and spin axis at 0° ecliptical longitude, 0° ecliptical latitude. Red angle reduced to $[0^\circ, +360^\circ]$, blue angles reduced to $[-180^\circ, +180^\circ]$.

It is worth to note that those angles do not depend on the kind of convention taken for the $\varphi_{\hat{P}}$ and the spin axis reference frame, as they are generated naturally from the geometry of $\hat{\mathbf{P}}_{\text{Ecl}}$ and $\hat{\mathbf{S}}$. So as an example at $\varphi_{\hat{P}} = 90^\circ, 180^\circ$ the scan circles are tangent to the local meridian if the spin axis is at right or left of the tangent point, automatically ψ takes values $+90^\circ$ and -90° . Also in this location ψ_{pol} slowly changes with $\varphi_{\hat{P}}$, while the opposite occurs at $\varphi_{\hat{P}} = 0^\circ$ and 180° . So as shown in Fig. 4, moving in anticlockwise direction from the South Ecliptic Pole to the South the ψ increases from 0° to 180° . At the South pole the angle switches and goes from -180° to -0° .

4.3 Spin axis on the ecliptic, Polarization S axis tilted with respect to $\hat{\mathbf{X}}_{\text{los}}$

Position and orientation of a beam in the LOS reference frame are encoded by three parameters in the optical database $\phi_{\text{uv}}, \theta_{\text{uv}}$ and ψ_{uv} . The corresponding transforming matrix $\mathbf{U}_{\text{det}}^{\text{ax}}(\phi_{\text{uv}}, \theta_{\text{uv}}, \psi_{\text{uv}})$ can be reduced to the product of three simple rotations in the LOS

$$\mathbf{U}_{\text{det}}^{\text{ax}}(\phi_{\text{uv}}, \theta_{\text{uv}}, \psi_{\text{uv}}) = \mathbf{R}_z(\delta\Phi)\mathbf{R}_y(\delta\Theta)\mathbf{R}_z(\hat{t}_X) \quad (7)$$



the effective angles at the right hand side of the equation are complicated functions of the $\phi_{uv}, \theta_{uv}, \psi_{uv}$ and their derivation is outside the scope of the present version of the document. It is sufficient to say that \hat{t}_X measures the the tilt of the $\hat{\mathbf{\Pi}}_S$ with respect to $\hat{\mathbf{X}}_{los}$ in the case $\phi_{uv} = 0^\circ$ and $\theta_{uv} = 0^\circ$, while $\delta\Phi$ and $\delta\Theta$ represents the variation of pointing direction of the beam with respect to that of the LOS.

To derive ψ the cases in which the $\hat{\mathbf{\Pi}}_S$ is tilted with respect to $\hat{\mathbf{X}}_{los}$, it is sufficient to consider the tilt angle $\hat{t}_X = \arccos(\hat{\mathcal{S}} \cdot \hat{\mathbf{\Pi}}_S)$ which is a function of ψ_{uv} , Θ_{det} and ϕ_{uv} .

$$\hat{\mathbf{\Pi}}_S = \cos \hat{t}_X \hat{\mathbf{s}} + \sin \hat{t}_X \hat{\mathbf{Y}}_{los}. \quad (8)$$

In our simplified case $\phi_{uv} = 0^\circ$, $\theta_{uv} = 0^\circ$ $\hat{t}_X = \psi_{uv}$ so that

$$\hat{\mathbf{\Pi}}_S = \cos \psi_{uv} \hat{\mathbf{s}} + \sin \psi_{uv} \hat{\mathbf{Y}}_{los}. \quad (9)$$

Then we redefine

$$\begin{aligned} \cos \psi_{pol,S} &= \hat{\mathbf{\Pi}}_S \cdot \hat{\mathcal{S}} \\ \sin \psi_{pol,S} &= (\hat{\mathcal{S}} \times \hat{\mathbf{\Pi}}_S) \cdot \hat{\mathbf{P}} \end{aligned} \quad (10)$$

Fig. 5 shows that the effect of $\hat{t}_X = \psi_{uv}$ is to shift up the ψ_{pol} curve as it increases. Tables from 3 to 6 lists values of ψ_{pol} for some relevant $\hat{t}_X = \psi_{uv}$ values.

4.4 Spin axis tilted on the ecliptic, Polarization S axis aligned with $\hat{\mathbf{X}}_{los}$

We consider a spin axis at 0° ecliptical latitude and at an ecliptical latitude b_{spin} . The new spin axis and $\hat{\mathbf{Z}}_{spin}$ are defined as:

$$\hat{\mathcal{S}}(b_{spin}) = \cos b_{spin} \hat{\mathbf{X}}_{ecl} + \sin b_{spin} \hat{\mathbf{Z}}_{ecl} \quad (11)$$

$$\hat{\mathbf{Z}}_{spin}(b_{spin}) = -\sin b_{spin} \hat{\mathbf{X}}_{ecl} + \cos b_{spin} \hat{\mathbf{Z}}_{ecl} \quad (12)$$

while of course the $\hat{\mathbf{Y}}_{spin}$ is not changed as it coincides with $\hat{\mathbf{Y}}_{ecl}$. Again $\hat{\mathbf{P}}(\varphi_{\hat{P}}) = \cos \varphi_{\hat{P}} \sin \beta \hat{\mathbf{Z}}_{spin} + \sin \varphi_{\hat{P}} \sin \beta \hat{\mathbf{Y}}_{spin} + \cos \varphi_{\hat{P}} \hat{\mathbf{X}}_{spin}$, so that it is easy to derive the new $\hat{\mathbf{P}}$ and $\hat{\mathbf{s}} = -\partial \hat{\mathbf{P}} / \partial \beta$, while the $\hat{\mathcal{S}}$ vector does not change.

The qualitative behaviour of ψ depends on the critical values $|b_{spin}| = 90^\circ - \beta$. In fact for $|b_{spin}| < 90^\circ - \beta$. the scan circle does not include neither the North nor the South ecliptical poles and the geometry of the problem does not change with respect to the case $b_{spin} = 0^\circ$ previously analyzed, see Fig. 6.

For $|b_{spin}| = 90^\circ - \beta$ either the North or the South pole are crossed by the circle. This restrict the possible values of ψ as shown in Fig. 7. In case $b_{spin} = 90^\circ - \beta$ never will happen that the $\hat{\mathcal{S}}$ pole is opposed to $\hat{\mathbf{s}}$ and so $-90^\circ \leq \psi \leq +90^\circ$, being 0° at the South Pole. On the contrary if $b_{spin} = -(90^\circ - \beta)$ it never happen that $\hat{\mathcal{S}}$ and $\hat{\mathbf{s}}$ are parallel so that the $-90^\circ \leq \psi \leq +90^\circ$ intervall is excluded.

For $|b_{spin}| > 90^\circ - \beta$ either the North or the South pole are enclosed in the circle. The qualitative behaviour of ψ is the same of the previous case apart from a smoother transition near the poles, see Fig. 8, but now the maximal elongation of the $\hat{\mathcal{S}}$ with respect to $\hat{\mathbf{s}}$ is less than 90° so that the intervall of variability for ψ is a bit less wider than $-90^\circ \leq \psi \leq +90^\circ$ or its complementar.

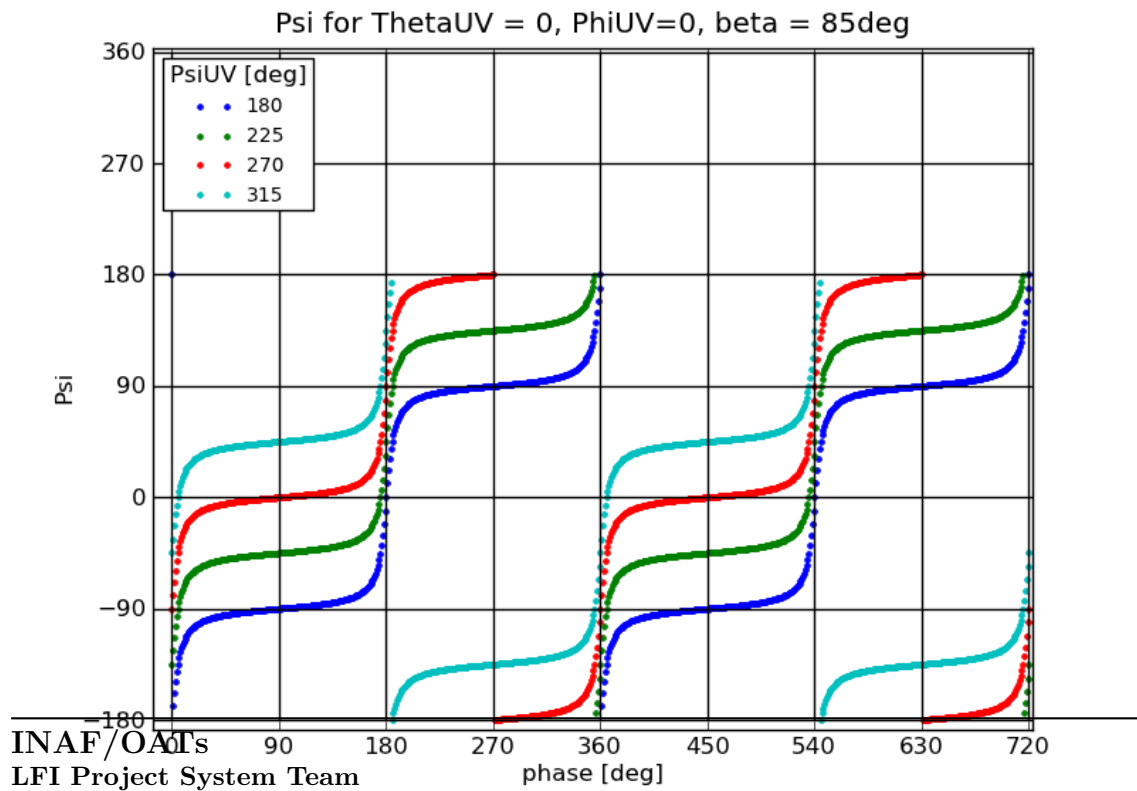
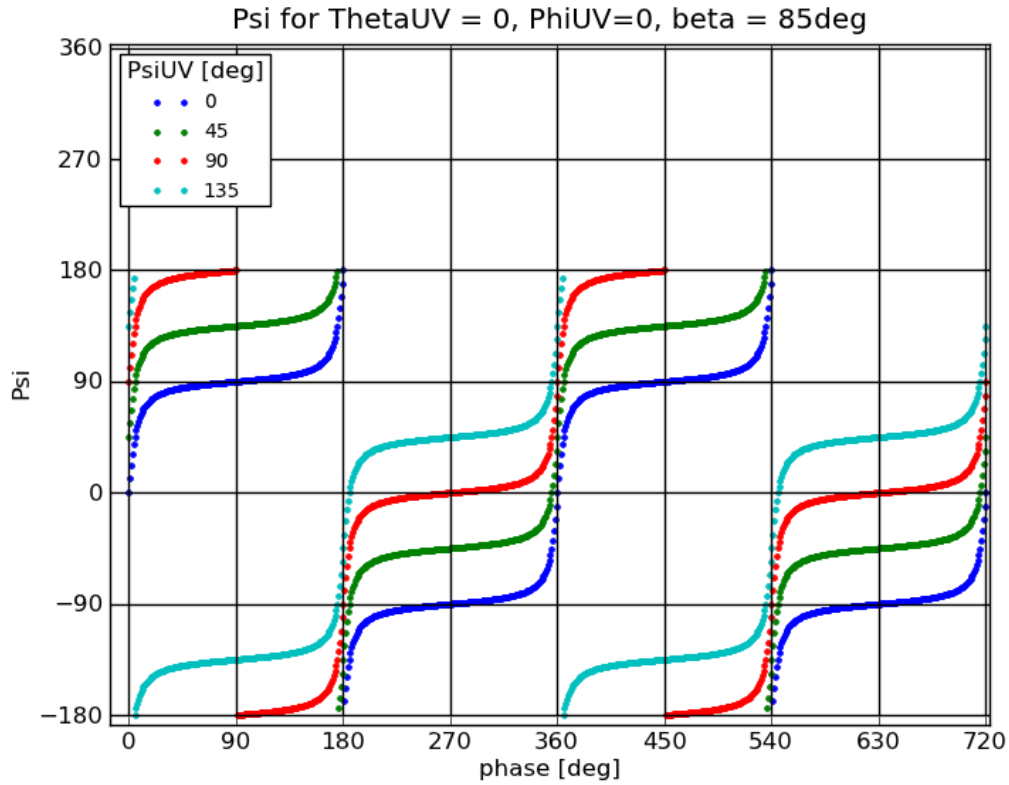


Figure 5

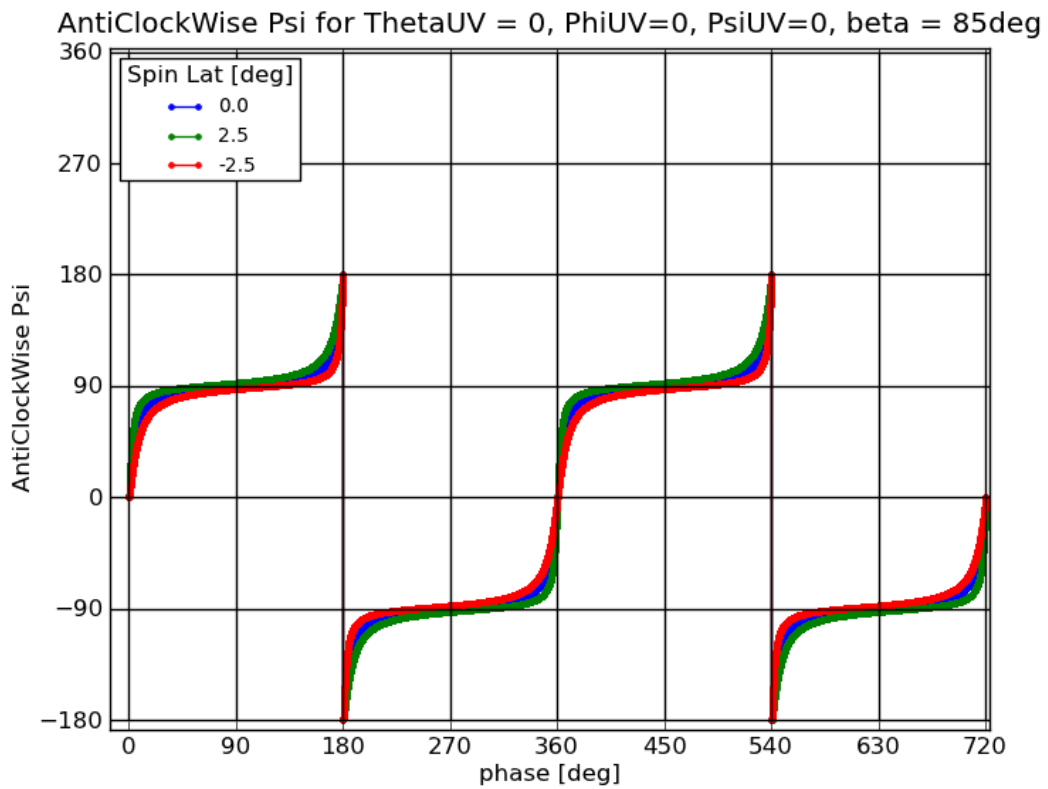


Figure 6

Values of ψ counted anticlockwise for $\beta = 85^\circ$ and spin axis at 0° ecliptical longitude, 0° ecliptical latitude varying b_{spin} with $|b_{\text{spin}}| < 90^\circ - \beta = 5^\circ$.

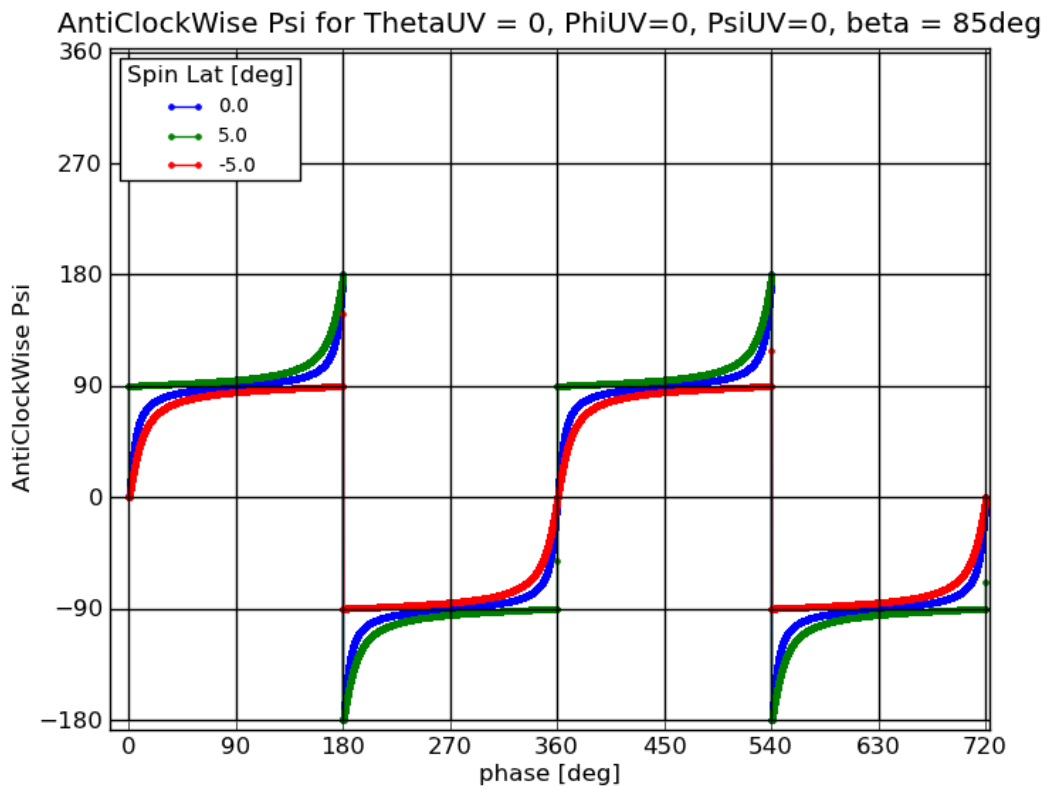


Figure 7

Values of ψ counted anticlockwise for $\beta = 85^\circ$ and spin axis at 0° ecliptical longitude, 0° ecliptical latitude for $b_{\text{spin}} = -5^\circ$ and $+5^\circ$.

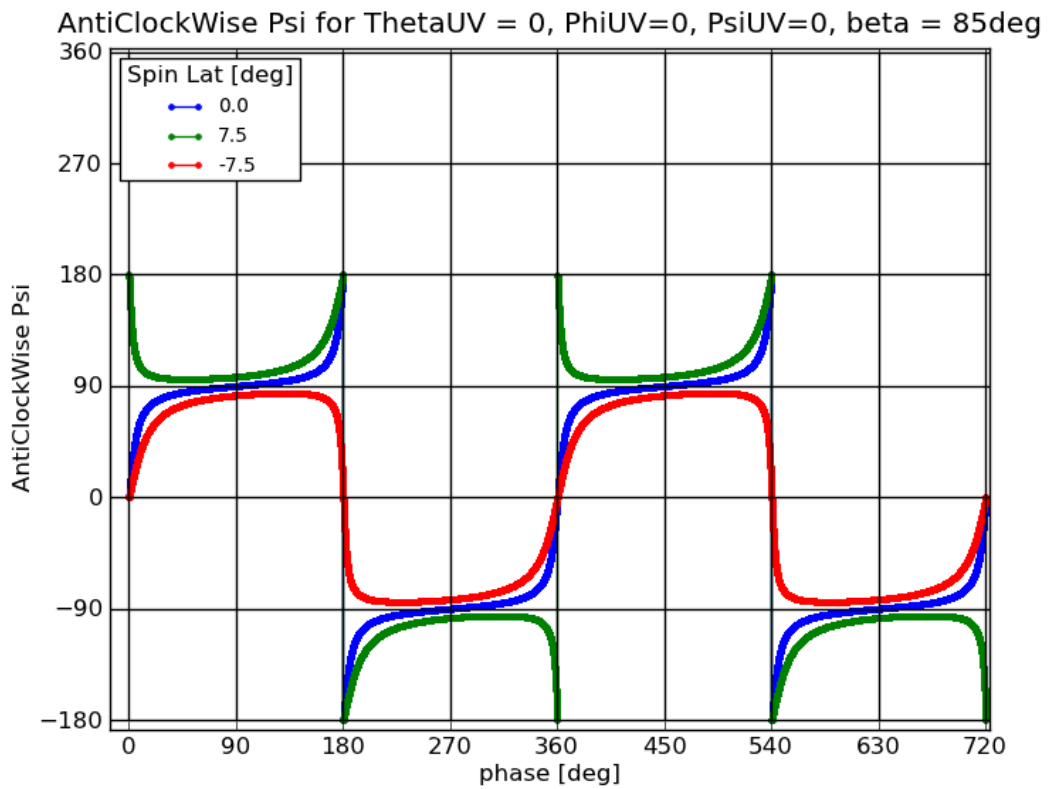


Figure 8

Values of ψ counted anticlockwise for $\beta = 85^\circ$ and spin axis at 0° ecliptical longitude, 0° ecliptical latitude for $b_{\text{spin}} = -7.5^\circ$ and $+7.5^\circ$.



4.5 ClockWise v.z. AntiClockWise

While the plots shown above does not depend wether the spacecraft rotates clockwise or anticlockwise. I.e. on the sign of $\varphi_{\hat{P}}$, of course it will depend wether if ψ is oriented to increase toward east or west, and wether the ecliptical sphere is seen from outside (pointing coming out from the tangent plane) or inside (pointing coming in the tangent plane), i.e. wether $\hat{\Pi}_S$ is counted clockwise or anticlockwise. The table below summarizes the various combinations

	$\hat{\Pi}_S$ increment Toward	
	East	West
Outside	clockwise	anticlockwise
Inside	anticlockwise	clockwise

since we assumed $\hat{\Pi}_S$ anticlockwise the clockwise case is simply obtained by reversing the sign of $\hat{\Pi}_S$.



5 Extracting beam attitude

Beam attitude information are reconstructed by using

1. Focal Plane database which describes how polarizations and beams are placed and oriented in the Focal Plane, and how the FP is related to the SpaceCraft structure.
2. Instantaneous attitude information provided by the attitude reconstruction system in form of quaternions, sampled at a constant rate t_{quat} .

The steps to compute \mathbf{psi} combining those information at a given sampling time t and given radiometer i_{det} are

1. Build the $\mathbf{U}_{\text{det}}^{\text{ax}}$ matrix converting beam polarization reference frame to LOS reference frame and then LOS reference frame SpaceCraft reference frame by using the telescope boresight angle β and the associated tuple of angles for the given radiometer $(\phi_{\text{uv}}, \theta_{\text{uv}}, \psi_{\text{uv}})$ (see Section 5.1).
2. interpolate quaternions at times t obtaining $\mathbf{Q}_{\text{sc}}(t)$
3. Build the attitude conversion matrix $\mathbf{Q}_{\text{SC}}^{\text{Ecl}}(\mathbf{Q}_{\text{sc}}(t))$ from the interpolated quaternion converting from the spacecraft reference frame to the Ecliptical Astrometric Reference Frame (Light Aberration not included).
4. Form the matrix transforming from the beam reference frame to the Ecliptical Astrometric Reference Frame (Light Aberration not included); (see Section 5.2).
5. extract Ecliptical Astrometric Pointing Coordinates (see Section 5.2).
6. Form rotation matrices for astrometric colatitude and longitude (see Section 5.3).
7. Compute the ψ (see Section 5.4).

5.1 Build the ax2det matrix

The $\mathbf{ax2det}$ matrix encodes a rotation from the Beam reference frame to the SpaceCraft reference frame and from LOS to SpaceCraft reference frame.

Conversion matrix from beam reference frame to LOS reference frame is performed by \mathbf{rotUV} matrix defined as

$$\mathbf{R}_{uv} = \mathbf{R}_z(90^\circ + \phi_{\text{uv}})\mathbf{R}_x(\theta_{\text{uv}})\mathbf{R}_z(-(90^\circ + \phi_{\text{uv}}))\mathbf{R}_z(\psi_{\text{uv}}). \quad (13)$$

The rotations for angles $\phi_{\text{uv}}, \theta_{\text{uv}}$ can be expressed also in a more compact form by using a Ludwig matrix [AD-2]¹

$$\mathbf{R}_{uv}^{\text{Ludwig}}(\theta_{\text{uv}}, \phi_{\text{uv}}) = \begin{pmatrix} 1 + \cos^2 \phi_{\text{uv}} (\cos \theta_{\text{uv}} - 1), & -\sin 2\phi_{\text{uv}} \sin^2(\theta_{\text{uv}}/2), & \cos \phi_{\text{uv}} \sin \theta_{\text{uv}} \\ -\sin 2\phi_{\text{uv}} \sin^2(\theta_{\text{uv}}/2), & 1 + \sin^2 \phi_{\text{uv}} (\cos \theta_{\text{uv}} - 1), & \sin \phi_{\text{uv}} \sin \theta_{\text{uv}} \\ -\cos \phi_{\text{uv}} \sin \theta_{\text{uv}}, & -\sin \phi_{\text{uv}} \sin \theta_{\text{uv}}, & \cos \theta_{\text{uv}} \end{pmatrix}. \quad (14)$$

¹The document has an error on the $\mathbf{R}_{uv}^{\text{Ludwig}}[x'][y']$ and $\mathbf{R}_{uv}^{\text{Ludwig}}[y'][x']$ which must be multiplied by -1 .



Conversion matrix from LOS to spacecraft reference frame.

$$\mathbf{M}_{\text{beta}} = \mathbf{R}_y(90^\circ - \beta) \quad (15)$$

At the end the `ax2det` matrix is defined as ²

$$\mathbf{U}_{\text{det}}^{\text{ax}} = \mathbf{M}_{\text{beta}} \mathbf{R}_{uv}. \quad (16)$$

The vector $\hat{\mathbf{S}}_{\text{pol}}^{\text{SC}}$ which is the versor of the S polarization vector in the spacecraft reference frame is given by the product

$$\hat{\mathbf{S}}_{\text{pol}}^{\text{SC}} = \mathbf{U}_{\text{det}}^{\text{ax}} \begin{pmatrix} 1 \\ 0 \\ 0 \end{pmatrix}; \quad (17)$$

while the direction in which the beam is directed with respect to the spacecraft is

$$\hat{\mathbf{P}}_{\text{SC}} = \mathbf{U}_{\text{det}}^{\text{ax}} \begin{pmatrix} 0 \\ 0 \\ 1 \end{pmatrix}. \quad (18)$$

5.2 Form the Attitude Conversion Matrix from Quaternions

At each time t_{quat} a quaternion $Q_{\text{sc}}(t_{\text{quat}})$ is provided by the AHF the quaternion is linearly interpolated in time and used to build an attitude rotation matrix $\mathbf{Q}_{\text{SC}}^{\text{Ecl}}(t)$ converting the SpaceCraft Reference Frame to the Ecliptical Reference Frame.

Quaternions do not include Light Aberration, so they provide Astrometric (i.e. Geometric) ecliptical coordinates.

The astrometric pointing direction of the beam at time t is defined by

$$\hat{\mathbf{P}}_{\text{Ecl,Ast}} = \mathbf{Q}_{\text{SC}}^{\text{Ecl}} \mathbf{U}_{\text{det}}^{\text{ax}} \begin{pmatrix} 0 \\ 0 \\ 1 \end{pmatrix}. \quad (19)$$

with $\hat{\mathbf{P}}_{\text{Ecl,Ast}}$ having components $(\hat{P}_{\text{Ecl,Ast,x}}, \hat{P}_{\text{Ecl,Ast,y}}, \hat{P}_{\text{Ecl,Ast,z}})$. The Astrometric Ecliptical Coordinates $\theta_{\text{Ecl,Ast}}$ and $\phi_{\text{Ecl,Ast}}$ are given by

$$\begin{aligned} \theta_{\text{Ecl,Ast}} &= \arccos(\hat{P}_{\text{Ecl,Ast,z}}) \\ \phi_{\text{Ecl,Ast}} &= \arctan2(\hat{P}_{\text{Ecl,Ast,y}}, \hat{P}_{\text{Ecl,Ast,x}}) \end{aligned} \quad (20)$$

5.3 Form rotation matrices for astrometric colatitude and longitude

Those matrices are used to transform the coordinates in the Astrometric Ecliptical reference frame to Ecliptical Coordinates centered on the beam.

$$\mathbf{R}_{\phi}^{\text{Ast}} = \mathbf{R}_z(-\phi_{\text{Ecl,Ast}}) = \begin{pmatrix} \cos \phi_{\text{Ecl,Ast}} & \sin \phi_{\text{Ecl,Ast}} & 0 \\ -\sin \phi_{\text{Ecl,Ast}} & \cos \phi_{\text{Ecl,Ast}} & 0 \\ 0 & 0 & 1 \end{pmatrix} \quad (21)$$

$$\mathbf{R}_{\theta}^{\text{Ast}} = \mathbf{R}_y(-(90^\circ - \theta_{\text{Ecl,Ast}})) = \begin{pmatrix} \cos(90^\circ - \theta_{\text{Ecl,Ast}}) & 0 & \sin(90^\circ - \theta_{\text{Ecl,Ast}}) \\ 0 & 1 & 0 \\ -\sin(90^\circ - \theta_{\text{Ecl,Ast}}) & 0 & \cos(90^\circ - \theta_{\text{Ecl,Ast}}) \end{pmatrix} \quad (22)$$

²See App. B for a numerical example derived from [AD-2].



5.4 Extract ψ

The ψ is extracted by forming the matrix

$$\mathbf{M}_{\text{Ecl,UV}} = \mathbf{R}_{\theta}^{\text{Ast}} \mathbf{R}_{\phi}^{\text{Ast}} \mathbf{Q}_{\text{SC}}^{\text{Ecl}} \mathbf{U}_{\text{det}}^{\text{ax}} \quad (23)$$

which represents the orientation of the S polarization axis in a reference frame drawn in the sky, centered on the beam and oriented with X axis along the local meridian and toward the Ecliptic North Pole.

Since the Z axis represents the pointing direction which for definition is $(0, 0, 1)$ vector then the matrix has the form

$$\mathbf{M}_{\text{Ecl,UV}} = \begin{pmatrix} a, & -b, & 0 \\ b, & a, & 0 \\ 0, & 0, & 1 \end{pmatrix} \quad (24)$$

with $a = \cos \psi$, $b = \sin \psi$.

So that

$$\psi = \arctan2(b, a). \quad (25)$$

The angle ψ so defined is

1. the rotation by which the S polarization axis has to be rotated in the plane tangent to the sphere in the pointing direction,
2. ψ is positive for anticlockwise rotation (the sphere being seen from outside, north at top)
3. ψ is zero when the S polarization axis points toward the Ecliptic South Pole along the local meridian



6 Usage of the angles: draw the polarization axis S and M

At a given time t we want to draw the polarization axis S and M at the location defined by the instantaneous pointing direction.

The input parameters are (θ, ϕ, ψ) .

Note that at the opposite of the previous section in this case θ and ϕ includes Light Aberration.

6.1 Step 1: form pointing matrices

$$\mathbf{R}_\phi = \begin{pmatrix} \cos \phi, & -\sin \phi, & 0 \\ \sin \phi, & \cos \phi, & 0 \\ 0, & 0, & 1 \end{pmatrix} \quad (26)$$

$$\mathbf{R}_\theta = \begin{pmatrix} \cos \theta, & 0, & \sin \theta \\ 0, & 1, & 0 \\ -\sin \theta, & 0, & \cos \theta \end{pmatrix} \quad (27)$$

6.2 Step 2: form local polarization matrices

$$\mathbf{M}_S = \begin{pmatrix} \cos(\psi + \psi_{\text{pol},S}), & -\sin(\psi + \psi_{\text{pol},S}), & 0 \\ \sin(\psi + \psi_{\text{pol},S}), & \cos(\psi + \psi_{\text{pol},S}), & 0 \\ 0, & 0, & 1 \end{pmatrix} \quad (28)$$

$$\mathbf{M}_M = \begin{pmatrix} \cos(\psi + \psi_{\text{pol},M}), & -\sin(\psi + \psi_{\text{pol},M}), & 0 \\ \sin(\psi + \psi_{\text{pol},M}), & \cos(\psi + \psi_{\text{pol},M}), & 0 \\ 0, & 0, & 1 \end{pmatrix} \quad (29)$$

Note that $\psi_{\text{pol},S} \equiv 0$ while $\psi_{\text{pol},M} \approx \pi/2$.

6.3 Step 3: form beam to ecliptical matrices

$$\mathbf{M}_S^{\text{Ecl}} = \mathbf{R}_\phi \mathbf{R}_\theta \mathbf{M}_S; \quad (30)$$

$$\mathbf{M}_M^{\text{Ecl}} = \mathbf{R}_\phi \mathbf{R}_\theta \mathbf{M}_M; \quad (31)$$

The pointing direction in aberrated Ecliptical Coordinates is given by both the two equations

$$\hat{\mathbf{P}} = \mathbf{M}_S^{\text{Ecl}} \begin{pmatrix} 0 \\ 0 \\ 1 \end{pmatrix}; \quad (32)$$

$$\hat{\mathbf{P}} = \mathbf{M}_M^{\text{Ecl}} \begin{pmatrix} 0 \\ 0 \\ 1 \end{pmatrix}. \quad (33)$$

The direction of the polarization S axis in the sky is instead given by

$$\hat{\mathbf{I}}_S^{\text{Ecl}} = \mathbf{M}_S^{\text{Ecl}} \begin{pmatrix} 1 \\ 0 \\ 0 \end{pmatrix}; \quad (34)$$



while for the M axis

$$\hat{\mathbf{n}}_M^{\text{Ecl}} = \mathbf{M}_M^{\text{Ecl}} \begin{pmatrix} 1 \\ 0 \\ 0 \end{pmatrix}. \quad (35)$$



7 Rotating a GRASP map

GRASP maps are already in the correct beam reference frame both for S and M (or X and Y) beams. Internal GRASP conventions assumes the Z axis of the map to coincide with the beam axis. Angles on the map not to behave as Euler angles. However, algorithm exists to convert those internal coordinates in usual colatitudes and longitudes. In particular a GRASP *cut* is a cut of the antenna electric field patterns along meridians, in slices of constant longitude $0^\circ \leq \Phi_{\text{GRASP}} \leq 180^\circ$ and variable polar coordinate $-180^\circ \leq \Theta_{\text{GRASP}} \leq +180^\circ$.

The conversion to usual polar coordinates is done by the equation

$$\begin{aligned}\Theta &= |\Theta_{\text{GRASP}}| \\ \Phi &= \Phi_{\text{GRASP}} \text{ if } \Theta_{\text{GRASP}} \geq 0^\circ \text{ else } \Phi_{\text{GRASP}} + 180^\circ;\end{aligned}\tag{36}$$

7.1 Total Power

For total power it is sufficient to use Eq. (30) to project a pixel in the GRASP map in the ecliptical reference frame or its inverse to project a pixel from the sky to the map.

7.2 Polarization

For polarization it has to be considered that electric fields has to be rotated. If $E_{\text{beam},x}$ and $E_{\text{beam},y}$ are the electric field components X and Y in the beam reference frame (usually complex numbers), the rotation of those fields in the ecliptic reference frame is accomplished by the following formula

$$\mathbf{E}_{\text{Ecl}} = \begin{pmatrix} 1 & 0 & 0 \\ 0 & 1 & 0 \\ 0 & 0 & 0 \end{pmatrix} \mathbf{M}_{\text{S}}^{\text{Ecl}} \begin{pmatrix} E_{\text{beam},x} \\ E_{\text{beam},y} \\ 0 \end{pmatrix}\tag{37}$$

where for a vector \mathbf{a} , $\hat{\mathbf{T}}_Z[\mathbf{a}] = \mathbf{a} - \mathbf{a} \cdot \hat{\mathbf{e}}_z \hat{\mathbf{e}}_z$.

However in general we are interested in the electric field components in the local reference frame, i.e. in the reference frame defined by $\hat{\mathbf{P}}_{\text{Ecl}}$, and the local meridian. In this case

$$\mathbf{E}_{\text{local}} = \begin{pmatrix} 1 & 0 & 0 \\ 0 & 1 & 0 \\ 0 & 0 & 0 \end{pmatrix} \mathbf{M}_{\text{S}} \begin{pmatrix} E_{\text{beam},x} \\ E_{\text{beam},y} \\ 0 \end{pmatrix}\tag{38}$$

the opposite case is also easily derived.



8 Converting between UV plane and polar coordinates

High resolution maps of beams are usually expressed in the (U, V) plane where U represents the X coordinate and V the Y coordinate.

The definition of the (U, V) is relative to the reference frame for which it is computed. Different reference frames will have different (U, V) planes, the most widely used (U, V) planes are the Beam and LOS (U, V) planes respectively defined for the Beam reference frame and the LOS reference frame.

If θ is the usual zenithal angle for the given reference frame and ϕ the azimuthal angle then a pointing direction in the given reference frame is defined as:

$$\hat{\mathbf{P}} = \sin \theta \cos \phi \hat{\mathbf{e}}_x + \sin \theta \sin \phi \hat{\mathbf{e}}_y + \cos \theta \hat{\mathbf{e}}_z. \quad (39)$$

The (U, V) plane is the projection of $\hat{\mathbf{P}}$ on the plane defined by $\hat{\mathbf{e}}_x, \hat{\mathbf{e}}_y$ of the given reference frame

$$\mathbf{P}_{UV} = U \hat{\mathbf{e}}_x + V \hat{\mathbf{e}}_y. \quad (40)$$

of course \mathbf{P}_{UV} is not a versor and

$$\begin{aligned} U &= \sin \theta \cos \phi, \\ V &= \sin \theta \sin \phi; \end{aligned} \quad (41)$$

The origin of the (U, V) plane is the projection of the $\hat{\mathbf{e}}_z$ axis of the given reference frame.

There is an inherent ambiguity in this definition, positions with equal ϕ but zenithal coordinates θ and $90^\circ - \theta$ will be projected onto the same (U, V) couple. However the (U, V) plane is used to represent the beam pattern near its origin so that always $\theta \leq 90^\circ$.

To convert back from (U, V) to the original reference frame (θ, ϕ) use

$$\begin{aligned} \phi &= \arctan2(V, U), \\ \theta &= \arcsin(U \cos \phi + V \sin \phi); \end{aligned} \quad (42)$$

where it is assumed that $\arctan2(0, 0) \equiv 0$ giving $\theta = 0$ for the origin and that $\theta \leq 90^\circ$.



9 Validating a Real Case

The strategy of validation with a real case is to take the beam axis in the Ecliptical Reference Frame for a given feed–horn and to project them back on the corresponding GRASP beam maps by just using the corresponding `detpoint_pol` information.

Since GRASP beam maps are easily linked to physical features of the spacecraft it is easy to decide whether the axis are properly projected from the sky to the map, also since beam axis are fixed on the map, the projected axis shall be invariant in time.

So the exercise is to take a well defined case where we have in ecliptical coordinates at a given time t the pointing direction $\hat{\mathbf{P}}_{\text{Ecl}}(t)$, the direction of the spin axis $\hat{\mathbf{S}}_{\text{Ecl}}(t)$ and the direction of the axis $\hat{\mathbf{V}}_{\text{Ecl}}(t) = \hat{\mathbf{P}}_{\text{Ecl}}(t) \times \hat{\mathbf{S}}_{\text{Ecl}}(t) / \sin \beta_{\text{fh}}$ with $\beta_{\text{fh}} = \arccos \hat{\mathbf{S}}_{\text{Ecl}}(t) \cdot \hat{\mathbf{P}}_{\text{Ecl}}(t)$ is the feed–horn boresight angle. Those versors can be projected in the beam reference frame giving three constant vectors

$$\begin{aligned}\hat{\mathbf{P}}_{\text{beam}} &= \mathbf{M}_{\text{S}}^{-1} \mathbf{R}_{\theta}^{-1} \mathbf{R}_{\phi}^{-1} \hat{\mathbf{P}}_{\text{Ecl}}(t); \\ \hat{\mathbf{S}}_{\text{beam}} &= \mathbf{M}_{\text{S}}^{-1} \mathbf{R}_{\theta}^{-1} \mathbf{R}_{\phi}^{-1} \hat{\mathbf{S}}_{\text{Ecl}}(t); \\ \hat{\mathbf{V}}_{\text{beam}} &= \mathbf{M}_{\text{S}}^{-1} \mathbf{R}_{\theta}^{-1} \mathbf{R}_{\phi}^{-1} \hat{\mathbf{V}}_{\text{Ecl}}(t);\end{aligned}\tag{43}$$

in particular the $\hat{\mathbf{S}}_{\text{beam}}$ vector shall fall more or less in the center, or very near the center, of the main spillover in the map at a colatitude equal to β_{fh} .

9.1 Selecting pointing period and samples

To simplify the analysis we look at a case where

1. the spin axis is as more as possible near the ecliptic;
2. the spin axis is stable;
3. the spin axis instantaneous coordinates can be replaced by time averaged coordinates;
4. the selected feed–horn has the minimal colatitude.

Conditions 2.) and 3.) requires to consider just the stability period, a simple check shows that during the stability period the spin axis oscillates at most of some tens of arcsec, so that condition 3.) is easily fulfilled. After inspecting the list of `AHF_info` we selected a pointing period of OD 167 where the spin axis is within 14 arcsec on the ecliptic. Tab. 1 gives the features of this pointing period.

9.2 Selecting the feed–horns

We considered FH 24 and 25. FH 24 is on the symmetry axis of the focal plane defined by the telescope LOS and the local direction of the spin axis, so that we are in a situation very similar to the one depicted in Section 4.2. FH 25 has its X axis making the largest angle with the LOS symmetry axis, i.e. nearly parallel to the scan direction.

9.3 Validating feed–horn 24

FH 24 is on the symmetry axis of the focal plane defined by the telescope LOS and the local direction of the spin axis, so that we are in a situation very similar to the one depicted in Section 4.2. Fig. 9 shows the geometry of the feed–horn, since its boresight angle $\beta_{\text{FH24}} \approx 88.58^\circ$ larger than

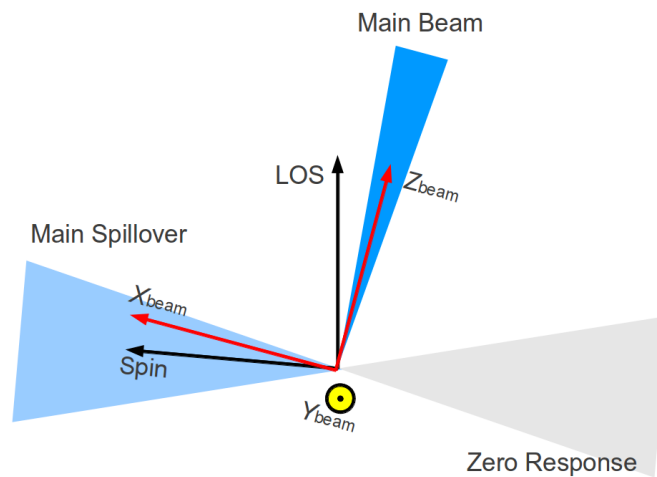


Figure 9: Geometry of feed-horn 24. The figure takes the plane which includes the Spin axis, the telescope LOS and the spin axis pointing direction. The main spillover is more or less located toward the spin axis, the region with zero response, due to the strong shielding produced by the V-Groves and the service module, is more or less opposed at the spin axis, the main beam points toward the Z of the beam reference frame.

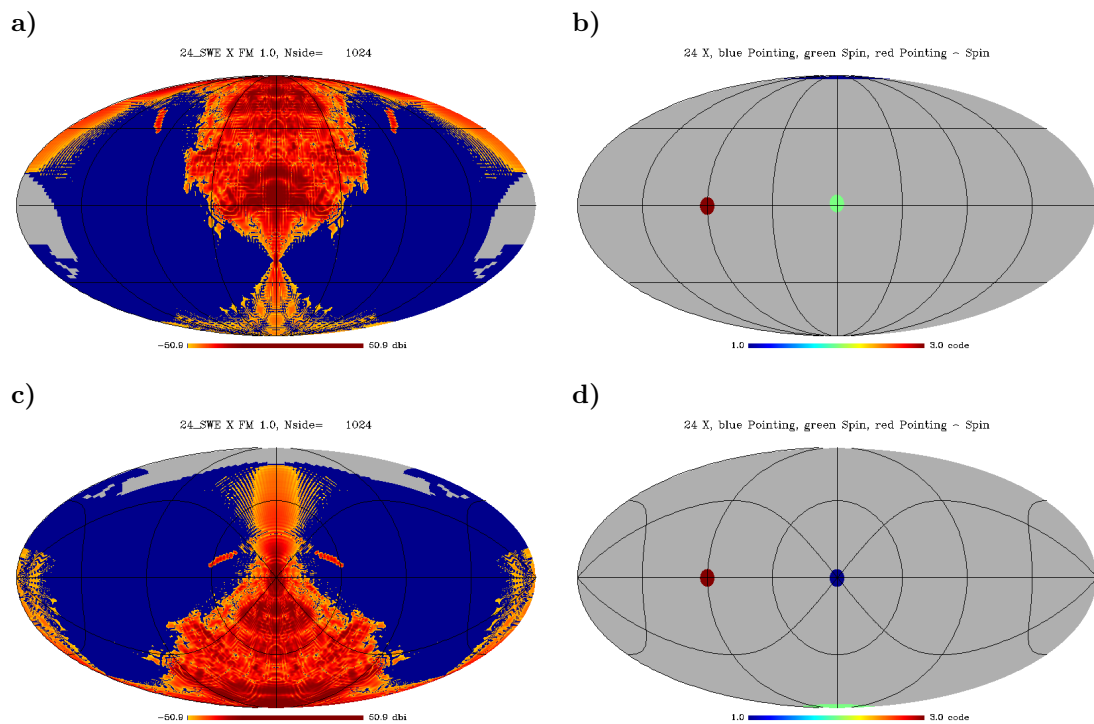


Figure 10: Validation of DMC processing for Feed-Horn 24. Frames a) and c) the GRASP map of beam power: a) seen from front ($Y > 0$ at mid of left side, X axis coming out from the center, Z axis at top) and c) seen from top ($Y > 0$ at mid of left side, Z axis coming out from the center, $X > 0$ axis at bottom). Frames b) and d) the spots represents the positions of $\hat{\mathbf{P}}$ (blue), $\hat{\mathbf{S}}$ (green), $\hat{\mathbf{P}} \times \hat{\mathbf{S}}$ (red) after rotation from the Ecliptical Reference Frame to the beam reference frame.



OD	167	
pointID_unique	2697	provided by the LFI/DPC
pointID_PSO	01032040	provided by the PSO
pointID_changes	381828	provided by the PSO
start_pID	1.07177812133617e+14	OBT of start maneuver
start_time	1.07177828157166e+14	OBT of start stability period
end_time	1.07177994258158e+14	OBT of end of stability period
midJD	2455132.80022311443463	Julian Day of mid stability period
SpinEclipticalLongitude	42.4761°	averaged from AHF over the stability period
SpinEclipticalLatitude	-0.004°	averaged from AHF over the stability period

Table 1: Features of the pointing period selected for the validation with the real case.

Sample	θ	ϕ
2229712	0.0249823008740562	0.939297060851545
2229713	0.0246386996614547	0.849640790471956
2229714	0.0244978016249136	0.758205742553804
2229715	0.0245631076834077	0.666488509019945
2229716	0.0248329909192899	0.576012807581414

Table 2: List of samples taken for the validation

85° the LOS is located between the Pointing direction (the $\hat{\mathbf{Z}}_{\text{beam}}$ axis) and the Spin axis. Fig. 10 shows the result of a test for sample 2229712 in Tab. 2. As expected the $\hat{\mathbf{P}}_{\text{beam}} \equiv \hat{\mathbf{Z}}_{\text{beam}}$, also the $\hat{\mathbf{S}}_{\text{beam}}$ falls in the main spillover and lies in the plane defined by $\hat{\mathbf{Z}}_{\text{beam}}$ and $\hat{\mathbf{X}}_{\text{beam}}$, and also $\hat{\mathbf{V}}_{\text{beam}} \equiv \hat{\mathbf{Y}}_{\text{beam}}$ as expected. Note that in the GRASP map the main spillover is in the positive side of the $\hat{\mathbf{X}}_{\text{beam}}$ axis and that the GRASP map is oriented to have $\hat{\mathbf{N}}_{\text{S}}$ directed toward the positive $\hat{\mathbf{X}}_{\text{beam}}$ i.e. toward the LOS and the spin axis. Identical results are obtained with the other samples, being the resulting rotated vectors constants.

9.4 Validating feed–horn 25

For Feed–Horn 25 the boresight angle is $\approx 82.14^\circ$ so that the $\hat{\mathbf{Z}}_{\text{beam}}$ is nearest to the spin axis than the LOS, also the feed horn has the maximal elongation outside the focal plane symmetry axis, so there will be substantial rotation about the $\hat{\mathbf{Z}}_{\text{beam}}$ axis.

Fig. 11 shows the geometry of $\hat{\mathbf{S}}_{\text{Ecl}}$, $\hat{\mathbf{P}}_{\text{Ecl}}$ and $\hat{\mathbf{V}}_{\text{Ecl}}$ after rotation in the beam reference frame. Again the spin axis is about in the middle of the main spillover. Also the LOS (not represented) is located near the meridian defined by $\hat{\mathbf{X}}_{\text{beam}}$ and the $\hat{\mathbf{Z}}_{\text{beam}}$ the $\hat{\mathbf{N}}_{\text{S}}$ is oriented toward the center of the focal plane.

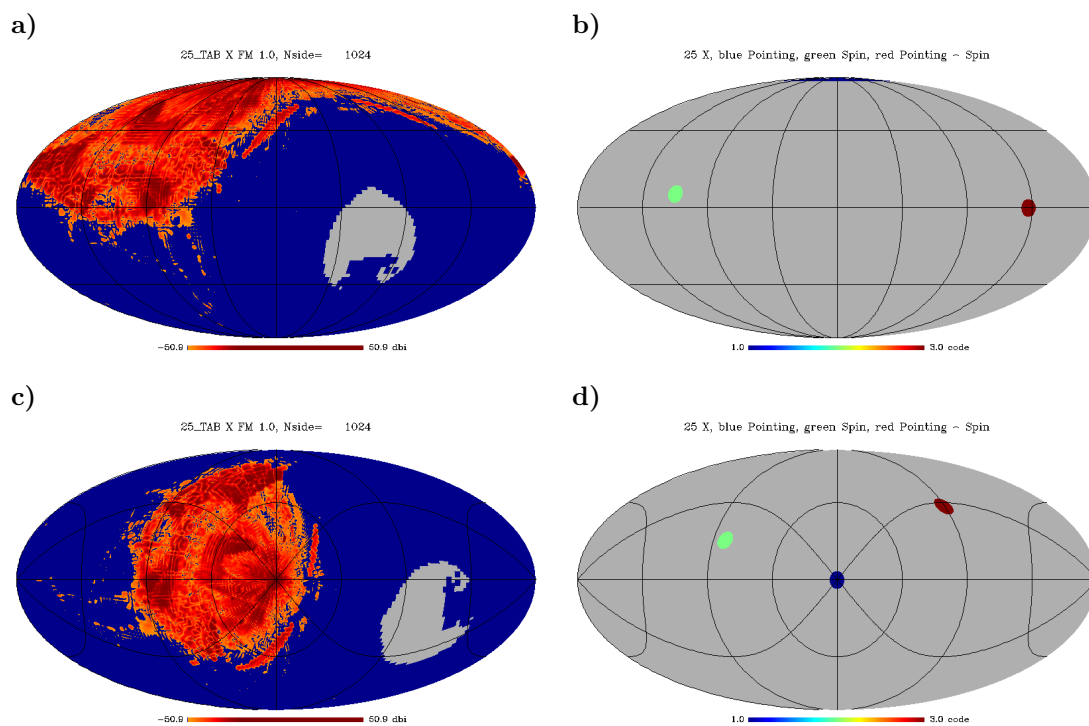


Figure 11: Validation of DMC processing for Feed-Horn 25. Frames a) and c) the GRASP map of beam power: a) seen from front ($Y > 0$ at mid of left side, X axis coming out from the center, Z axis at top) and c) seen from top ($Y > 0$ at mid of left side, Z axis coming out from the center, $X > 0$ axis at bottom). Frames b) and d) the spots represents the positions of $\hat{\mathbf{P}}$ (blue), $\hat{\mathbf{S}}$ (green), $\hat{\mathbf{P}} \times \hat{\mathbf{S}}$ (red) after rotation from the Ecliptical Reference Frame to the beam reference frame.



A Reference Frames

This appendix describes in detail the reference frames used in this document.

All the the reference frames are

1. right handed;
2. drawn on the unit sphere;
3. described as seen from outside;
4. the zenithal coordinates are taken from the pole drawn at north;
5. when looking at a tangent plane to the unit sphere on the location $\hat{\mathbf{P}}$ it is assumed $\hat{\mathbf{P}}$ is seen coming out from the sphere toward the observer;
6. the positive rotation direction for angles is AntiClockWise;

A.1 IAU Astrometric Ecliptical Reference Frame

Role used to describe the absolute location, pointing and orientation of PLANCK;

Origin the invariant Solar System Baricenter (SSB);

Fundamental Plane the plane of ecliptic at Year 2000 (J2000);

Polar Axis $\hat{\mathbf{Z}}_{\text{ecl}}$ the axis normal to ecliptic oriented toward the ecliptic North Pole;

Plane Axis $\hat{\mathbf{X}}_{\text{ecl}}, \hat{\mathbf{Y}}_{\text{ecl}}$

$\hat{\mathbf{X}}_{\text{ecl}}$ aligned with the vernal equinox at Year 2000;

$$\hat{\mathbf{Y}}_{\text{ecl}} = \hat{\mathbf{Z}}_{\text{ecl}} \times \hat{\mathbf{X}}_{\text{ecl}}$$

Coordinates (ℓ°, b°)

b° counted from the equator, positive toward the North Pole;

ℓ° counted along the equator from $\hat{\mathbf{X}}_{\text{ecl}}$ increasing anticlockwise.

A.2 COSMO Ecliptical Reference Frame

It is equivalent at the IAU R.F. but with a different definition of coordinates

Role used to describe the absolute location, pointing and orientation of PLANCK;

Origin the invariant Solar System Baricenter (SSB);

Fundamental Plane the plane of ecliptic at Year 2000 (J2000);

Polar Axis $\hat{\mathbf{Z}}_{\text{ecl}}$ the axis normal to ecliptic oriented toward the ecliptic North Pole;

Plane Axis $\hat{\mathbf{X}}_{\text{ecl}}, \hat{\mathbf{Y}}_{\text{ecl}}$

$\hat{\mathbf{X}}_{\text{ecl}}$ aligned with the vernal equinox at Year 2000;

$$\hat{\mathbf{Y}}_{\text{ecl}} = \hat{\mathbf{Z}}_{\text{ecl}} \times \hat{\mathbf{X}}_{\text{ecl}}$$

Coordinates (ϕ, θ)

$\theta = 90^\circ - b^\circ$ colatitude, counted from the from the North Pole.

ϕ longitude, defined as ℓ° , counted along the equator from $\hat{\mathbf{X}}_{\text{ecl}}$ increasing anticlockwise.



A.3 Spin Axis Reference Frame

Role used to describe the rotation of PLANCK during the stable pointing period;

Origin the spacecraft center of mass;

Fundamental Plane the plane normal to the PLANCK rotation axis (ideally the spin axis);

Polar Axis $\hat{\mathbf{X}}_{\text{spin}}$ the spin axis;

Plane Axis $\hat{\mathbf{Z}}_{\text{spin}}, \hat{\mathbf{Y}}_{\text{spin}}$

$\hat{\mathbf{Z}}_{\text{spin}}$ normal to $\hat{\mathbf{X}}_{\text{spin}}$ in the plane defined by the telescope LOS and the spin axis;

$$\hat{\mathbf{Y}}_{\text{spin}} = \hat{\mathbf{Z}}_{\text{spin}} \times \hat{\mathbf{X}}_{\text{spin}}$$

Coordinates specific spherical coordinates are not currently defined

A.4 SpaceCraft Reference Frame

Role used to described the relative orientation of optical and mechanical parts of PLANCK;

Origin the spacecraft center of mass;

Fundamental Plane the plane normal to the PLANCK main axis (ideally the spin axis);

Polar Axis $\hat{\mathbf{X}}_{\text{spin}}$ the spin axis;

Plane Axis $\hat{\mathbf{Z}}_{\text{spin}}, \hat{\mathbf{Y}}_{\text{spin}}$

$\hat{\mathbf{Z}}_{\text{spin}}$ normal to $\hat{\mathbf{X}}_{\text{spin}}$ in the plane defined by the telescope LOS and the spin axis;

$$\hat{\mathbf{Y}}_{\text{spin}} = \hat{\mathbf{Z}}_{\text{spin}} \times \hat{\mathbf{X}}_{\text{spin}}$$

Coordinates specific spherical coordinates are not currently defined

A.5 Telescope Reference Frame (also LOS RF)

Role used to described the relative location and orientation of beams in the Focal Plane;

Origin the spacecraft center of mass;

Fundamental Plane the plane normal to the telescope Line of Sight (LOS);

Polar Axis $\hat{\mathbf{Z}}_{\text{los}}$ the telescope line of sight;

Plane Axis $\hat{\mathbf{X}}_{\text{los}}, \hat{\mathbf{Y}}_{\text{los}}$

$\hat{\mathbf{X}}_{\text{los}}$ normal to $\hat{\mathbf{Z}}_{\text{los}}$ in the plane defined by the telescope LOS and the spin axis, directed toward the spin axis;

$\hat{\mathbf{Y}}_{\text{los}} = \hat{\mathbf{Z}}_{\text{los}} \times \hat{\mathbf{X}}_{\text{los}}$, parallel to the scan direction, positive toward the scan direction;

Coordinates $(\Phi_{\text{los}}, \Theta_{\text{los}})$

$\Theta_{\text{los}} = \arccos \hat{\mathbf{P}} \cdot \hat{\mathbf{Z}}_{\text{los}}$ angular distance from the LOS;

Φ_{los} longitude, counted from the $\hat{\mathbf{X}}_{\text{los}}$ increasing anticlockwise.



A.6 Beam Reference Frame

Role used to describe the optical properties of the beam;

Origin the spacecraft center of mass;

Fundamental Plane the plane normal to the beam main axis;

Polar Axis $\hat{\mathbf{Z}}_{\text{beam}}$ the beam main axis, so $\hat{\mathbf{P}} = \hat{\mathbf{Z}}_{\text{beam}}$;

Plane Axis $\hat{\mathbf{X}}_{\text{beam}}, \hat{\mathbf{Y}}_{\text{beam}}$

$\hat{\mathbf{X}}_{\text{beam}}$ normal to $\hat{\mathbf{Z}}_{\text{beam}}$ aligned with the *S* polarization axis $\hat{\mathbf{\Pi}}_S$;

$\hat{\mathbf{Y}}_{\text{beam}} = \hat{\mathbf{Z}}_{\text{beam}} \times \hat{\mathbf{X}}_{\text{beam}}$;

Coordinates (Φ, Θ)

$\cos \Theta = \hat{\mathbf{P}} \cdot \hat{\mathbf{Z}}_{\text{beam}}$ angular distance from the beam axis;

Φ longitude, counted from the $\hat{\mathbf{X}}_{\text{beam}}$ increasing anticlockwise.

Notes: It is conventionally assumed also

$\hat{\mathbf{P}}_{\text{Ecl}}$ is the pointing vector in the ecliptic;

$\hat{\mathbf{\Pi}}_S^{\text{Ecl}}$ the already mentioned polarization *S* axis;

$\hat{\mathbf{\Pi}}_M^{\text{Ecl}}$ the polarization *M* axis;

$\hat{\mathbf{B}}_a^{\text{Ecl}}$ the major axis of the main beam in the elliptical gaussian approximation.

$\hat{\mathbf{\Pi}}_S^{\text{Ecl}}, \hat{\mathbf{\Pi}}_M^{\text{Ecl}}$ and $\hat{\mathbf{B}}_a^{\text{Ecl}}$ are coplanar and normal to $\hat{\mathbf{P}}_{\text{Ecl}}$.

The angles ψ_{pol} and ψ_{ell} are measured in the tangent plane seen from outside the sphere.



B Two examples of validation of the ax2det matrix

We derive two validation examples for the `ax2det` matrix.

First Example This is based on the [AD-2]

$$\begin{aligned} & \mathbf{U}_{\text{det}}^{\text{ax}} (\beta = 80^\circ, \phi_{\text{uv}} = 126.0274^\circ, \theta_{\text{uv}} = 5.62^\circ, \phi_{\text{uv}} = 0^\circ) = \\ & = \begin{pmatrix} 0.99317225848691, & -0.01150118379631, & 0.11608870635553 \\ 0.00228644214044, & 0.996856145127, & 0.07919973551008 \\ -0.11663463102508, & -0.07839355007788, & 0.99007616583363 \end{pmatrix} \end{aligned}$$

Second Example This is derived by validating the \mathbf{R}_{uv}^{-1} matrix against GRASP9.

$$\begin{aligned} & \mathbf{R}_{uv}^{-1} (\phi_{\text{uv}} = -131.81796^\circ, \theta_{\text{uv}} = 3.32176^\circ, \phi_{\text{uv}} = 22.20^\circ) = \\ & = \begin{pmatrix} 0.92486356115532997, & 0.37671520243118273, & 0.052086941783083637 \\ -0.37833155437841293, & 0.92532203731490692, & 0.025384290831222921 \\ -0.038634546829169739, & -0.043183139263179356, & 0.99831988274033767 \end{pmatrix} \\ & \mathbf{U}_{\text{det}}^{\text{ax}} (\beta = 85^\circ, \phi_{\text{uv}} = -131.81796^\circ, \theta_{\text{uv}} = 3.32176^\circ, \phi_{\text{uv}} = 22.20^\circ) = \\ & = \begin{pmatrix} 0.92588385217974911, & -0.3746795018710663, & 0.04852178016559297 \\ 0.37671520243118295, & 0.92532203731490659, & -0.043183139263179342 \\ -0.028718435368615618, & 0.058261463567609778, & 0.99788819681011287 \end{pmatrix} \end{aligned}$$

C Calculations and tables for the first validation example

In this appendix details for the calculation of angles in some notable cases are reported. Here $\beta = 85^\circ$, $C_\beta = \cos \beta$ and $S_\beta = \sin \beta$.

$$\varphi_{\hat{P}} = 0^\circ$$

$$\begin{aligned} \hat{\mathbf{P}}_{\text{Ecl}} &= C_\beta \hat{\mathbf{X}}_{\text{ecl}} + S_\beta \hat{\mathbf{Z}}_{\text{ecl}} \\ \hat{\mathbf{X}}_{\text{los}}^{\text{ecl}} &= -S_\beta \hat{\mathbf{X}}_{\text{ecl}} - C_\beta \hat{\mathbf{Z}}_{\text{ecl}} \\ \hat{\mathbf{Y}}_{\text{los}}^{\text{ecl}} &= \hat{\mathbf{Y}}_{\text{ecl}} \\ \theta &= \arccos \sin \beta = 90^\circ - \beta = 5^\circ \\ \phi &= 0^\circ \\ \psi &= 0^\circ \end{aligned}$$

$$\varphi_{\hat{P}} = 45^\circ$$

$$\begin{aligned} \hat{\mathbf{P}}_{\text{Ecl}} &= C_\beta \hat{\mathbf{X}}_{\text{ecl}} - 1/\sqrt{2} S_\beta \hat{\mathbf{Y}}_{\text{ecl}} + 1/\sqrt{2} S_\beta \hat{\mathbf{Z}}_{\text{ecl}} \\ \hat{\mathbf{X}}_{\text{los}}^{\text{ecl}} &= S_\beta \hat{\mathbf{X}}_{\text{ecl}} + 1/\sqrt{2} C_\beta \hat{\mathbf{Y}}_{\text{ecl}} - 1/\sqrt{2} C_\beta \hat{\mathbf{Z}}_{\text{ecl}} \\ \hat{\mathbf{Y}}_{\text{los}}^{\text{ecl}} &= 1/\sqrt{2} \hat{\mathbf{Y}}_{\text{ecl}} + 1/\sqrt{2} \hat{\mathbf{Z}}_{\text{ecl}} \\ \Theta &= \arccos(1/\sqrt{2} S_\beta) = 45.21761^\circ \\ \Phi &= -\arctan 2(S_\beta, \sqrt{2} C_\beta) = 277.05323^\circ \\ \psi &= +85.01893^\circ \end{aligned}$$



$$\varphi_{\hat{P}} = 90^\circ$$

$$\begin{aligned}\hat{\mathbf{P}}_{\text{Ecl}} &= C_\beta \hat{\mathbf{X}}_{\text{ecl}} - S_\beta \hat{\mathbf{Y}}_{\text{ecl}} \\ \hat{\mathbf{X}}_{\text{los}}^{\text{ecl}} &= S_\beta \hat{\mathbf{X}}_{\text{ecl}} + C_\beta \hat{\mathbf{Y}}_{\text{ecl}} \\ \hat{\mathbf{Y}}_{\text{los}}^{\text{ecl}} &= \hat{\mathbf{Z}}_{\text{ecl}} \\ \Theta &= 90^\circ \\ \Phi &= 360^\circ - \beta = 275^\circ \\ \psi &= +90^\circ\end{aligned}$$

$$\varphi_{\hat{P}} = 135^\circ$$

$$\begin{aligned}\hat{\mathbf{P}}_{\text{Ecl}} &= C_\beta \hat{\mathbf{X}}_{\text{ecl}} - 1/\sqrt{2} S_\beta \hat{\mathbf{Y}}_{\text{ecl}} - 1/\sqrt{2} S_\beta \hat{\mathbf{Z}}_{\text{ecl}} \\ \hat{\mathbf{X}}_{\text{los}}^{\text{ecl}} &= S_\beta \hat{\mathbf{X}}_{\text{ecl}} + 1/\sqrt{2} C_\beta \hat{\mathbf{Y}}_{\text{ecl}} + 1/\sqrt{2} C_\beta \hat{\mathbf{Z}}_{\text{ecl}} \\ \hat{\mathbf{Y}}_{\text{los}}^{\text{ecl}} &= -1/\sqrt{2} \hat{\mathbf{Y}}_{\text{ecl}} + 1/\sqrt{2} \hat{\mathbf{Z}}_{\text{ecl}} \\ \Theta &= \arccos(-1/\sqrt{2} S_\beta) = 134.78238^\circ \\ \Phi &= -\arctan 2(S_\beta, \sqrt{2} C_\beta) = 277.05323^\circ \\ \psi &= +94.98107^\circ\end{aligned}$$

$$\varphi_{\hat{P}} = 180^\circ$$

$$\begin{aligned}\hat{\mathbf{P}}_{\text{Ecl}} &= C_\beta \hat{\mathbf{X}}_{\text{ecl}} - S_\beta \hat{\mathbf{Z}}_{\text{ecl}} \\ \hat{\mathbf{X}}_{\text{los}}^{\text{ecl}} &= S_\beta \hat{\mathbf{X}}_{\text{ecl}} + C_\beta \hat{\mathbf{Z}}_{\text{ecl}} \\ \hat{\mathbf{Y}}_{\text{los}}^{\text{ecl}} &= -\hat{\mathbf{Y}}_{\text{ecl}} \\ \Theta &= \arccos(-\sin \beta) = 90^\circ + \beta = 175^\circ \\ \Phi &= 0^\circ \\ \psi &= +180^\circ\end{aligned}$$

$$\varphi_{\hat{P}} = 225^\circ$$

$$\begin{aligned}\hat{\mathbf{P}}_{\text{Ecl}} &= C_\beta \hat{\mathbf{X}}_{\text{ecl}} + 1/\sqrt{2} S_\beta \hat{\mathbf{Y}}_{\text{ecl}} - 1/\sqrt{2} S_\beta \hat{\mathbf{Z}}_{\text{ecl}} \\ \hat{\mathbf{X}}_{\text{los}}^{\text{ecl}} &= S_\beta \hat{\mathbf{X}}_{\text{ecl}} - 1/\sqrt{2} C_\beta \hat{\mathbf{Y}}_{\text{ecl}} + 1/\sqrt{2} C_\beta \hat{\mathbf{Z}}_{\text{ecl}} \\ \hat{\mathbf{Y}}_{\text{los}}^{\text{ecl}} &= -1/\sqrt{2} \hat{\mathbf{Y}}_{\text{ecl}} - 1/\sqrt{2} \hat{\mathbf{Z}}_{\text{ecl}} \\ \Theta &= \arccos(-1/\sqrt{2} S_\beta) = 134.78238^\circ \\ \Phi &= \arctan 2(S_\beta, \sqrt{2} C_\beta) = 82.94677^\circ \\ \psi &= -94.98107^\circ\end{aligned}$$

$$\varphi_{\hat{P}} = 270^\circ$$

$$\begin{aligned}\hat{\mathbf{P}}_{\text{Ecl}} &= C_\beta \hat{\mathbf{X}}_{\text{ecl}} + S_\beta \hat{\mathbf{Y}}_{\text{ecl}} \\ \hat{\mathbf{X}}_{\text{los}}^{\text{ecl}} &= S_\beta \hat{\mathbf{X}}_{\text{ecl}} - C_\beta \hat{\mathbf{Y}}_{\text{ecl}} \\ \hat{\mathbf{Y}}_{\text{los}}^{\text{ecl}} &= -\hat{\mathbf{Z}}_{\text{ecl}} \\ \Theta &= 90^\circ \\ \Phi &= 85^\circ \\ \psi &= -90^\circ\end{aligned}$$



$$\varphi_{\hat{P}} = 315^\circ$$

$$\begin{aligned}\hat{\mathbf{P}}_{\text{Ecl}} &= C_\beta \hat{\mathbf{X}}_{\text{ecl}} + 1/\sqrt{2} S_\beta \hat{\mathbf{Y}}_{\text{ecl}} + 1/\sqrt{2} S_\beta \hat{\mathbf{Z}}_{\text{ecl}} \\ \hat{\mathbf{X}}_{\text{los}}^{\text{ecl}} &= S_\beta \hat{\mathbf{X}}_{\text{ecl}} - 1/\sqrt{2} C_\beta \hat{\mathbf{Y}}_{\text{ecl}} - 1/\sqrt{2} C_\beta \hat{\mathbf{Z}}_{\text{ecl}} \\ \hat{\mathbf{Y}}_{\text{los}}^{\text{ecl}} &= 1/\sqrt{2} * Y_{\text{ecl}} - 1/\sqrt{2} \hat{\mathbf{Z}}_{\text{ecl}} \\ \Theta &= \arccos(1/\sqrt{2} S_\beta) = 45.21761^\circ \\ \Phi &= \arctan2(S_\beta, \sqrt{2} C_\beta) = 82.94677 \\ \psi &= -85.01893^\circ\end{aligned}$$



D Tables

$\psi_{uv} = 0^\circ$				
$\varphi_{\hat{p}}$	ϕ	θ	ψ [$-180^\circ, +180^\circ$]	ψ [$0^\circ, 360^\circ$]
0	-0.00000	5.00000	0.00000	0.00000
45	-82.94677	45.21762	85.01893	85.01893
90	-85.00000	90.00000	90.00000	90.00000
135	-82.94677	134.78238	94.98107	94.98107
180	-0.00000	175.00000	180.00000	180.00000
225	82.94677	134.78238	-94.98107	265.01893
270	85.00000	90.00000	-90.00000	270.00000
315	82.94677	45.21762	-85.01893	274.98107
360	0.00000	5.00000	-0.00000	360.00000

$\psi_{uv} = 45^\circ$				
$\varphi_{\hat{p}}$	ϕ	θ	ψ [$-180^\circ, +180^\circ$]	ψ [$0^\circ, 360^\circ$]
0	-0.00000	5.00000	45.00000	45.00000
45	-82.94677	45.21762	130.01893	130.01893
90	-85.00000	90.00000	135.00000	135.00000
135	-82.94677	134.78238	139.98107	139.98107
180	-0.00000	175.00000	-135.00000	225.00000
225	82.94677	134.78238	-49.98107	310.01893
270	85.00000	90.00000	-45.00000	315.00000
315	82.94677	45.21762	-40.01893	319.98107
360	0.00000	5.00000	45.00000	45.00000

Table 3: Table of ψ for $\psi_{uv} = 0^\circ$ and $\psi_{uv} = 45^\circ$.



$\psi_{uv} = 90^\circ$

$\varphi_{\hat{p}}$	ϕ	θ	ψ	
			$[-180^\circ, +180^\circ]$	$[0^\circ, 360^\circ]$
0	-0.00000	5.00000	90.00000	90.00000
45	-82.94677	45.21762	175.01893	175.01893
90	-85.00000	90.00000	180.00000	180.00000
135	-82.94677	134.78238	-175.01893	184.98107
180	-0.00000	175.00000	-90.00000	270.00000
225	82.94677	134.78238	-4.98107	355.01893
270	85.00000	90.00000	-0.00000	360.00000
315	82.94677	45.21762	4.98107	4.98107
360	0.00000	5.00000	90.00000	90.00000

$\psi_{uv} = 135^\circ$

$\varphi_{\hat{p}}$	ϕ	θ	ψ	
			$[-180^\circ, +180^\circ]$	$[0^\circ, 360^\circ]$
0	-0.00000	5.00000	135.00000	135.00000
45	-82.94677	45.21762	-139.98107	220.01893
90	-85.00000	90.00000	-135.00000	225.00000
135	-82.94677	134.78238	-130.01893	229.98107
180	-0.00000	175.00000	-45.00000	315.00000
225	82.94677	134.78238	40.01893	40.01893
270	85.00000	90.00000	45.00000	45.00000
315	82.94677	45.21762	49.98107	49.98107
360	0.00000	5.00000	135.00000	135.00000

Table 4: Table of ψ for $\psi_{uv} = 90^\circ$ and $\psi_{uv} = 135^\circ$.



$\psi_{uv} = 180^\circ$				
$\varphi_{\hat{P}}$	ϕ	θ	ψ	
			$[-180^\circ, +180^\circ]$	$[0^\circ, 360^\circ]$
0	-0.00000	5.00000	180.00000	180.00000
45	-82.94677	45.21762	-94.98107	265.01893
90	-85.00000	90.00000	-90.00000	270.00000
135	-82.94677	134.78238	-85.01893	274.98107
180	-0.00000	175.00000	-0.00000	360.00000
225	82.94677	134.78238	85.01893	85.01893
270	85.00000	90.00000	90.00000	90.00000
315	82.94677	45.21762	94.98107	94.98107
360	0.00000	5.00000	180.00000	180.00000

$\psi_{uv} = 225^\circ$				
$\varphi_{\hat{P}}$	ϕ	θ	ψ	
			$[-180^\circ, +180^\circ]$	$[0^\circ, 360^\circ]$
0	-0.00000	5.00000	-135.00000	225.00000
45	-82.94677	45.21762	-49.98107	310.01893
90	-85.00000	90.00000	-45.00000	315.00000
135	-82.94677	134.78238	-40.01893	319.98107
180	-0.00000	175.00000	45.00000	45.00000
225	82.94677	134.78238	130.01893	130.01893
270	85.00000	90.00000	135.00000	135.00000
315	82.94677	45.21762	139.98107	139.98107
360	0.00000	5.00000	-135.00000	225.00000

Table 5: Table of ψ for $\psi_{uv} = 180^\circ$ and $\psi_{uv} = 225^\circ$.



$\psi_{uv} = 270^\circ$				
$\varphi_{\hat{p}}$	ϕ	θ	ψ	
			$[-180^\circ, +180^\circ]$	$[0^\circ, 360^\circ]$
0	-0.00000	5.00000	-90.00000	270.00000
45	-82.94677	45.21762	-4.98107	355.01893
90	-85.00000	90.00000	-0.00000	360.00000
135	-82.94677	134.78238	4.98107	4.98107
180	-0.00000	175.00000	90.00000	90.00000
225	82.94677	134.78238	175.01893	175.01893
270	85.00000	90.00000	180.00000	180.00000
315	82.94677	45.21762	-175.01893	184.98107
360	0.00000	5.00000	-90.00000	270.00000

$\psi_{uv} = 315^\circ$				
$\varphi_{\hat{p}}$	ϕ	θ	ψ	
			$[-180^\circ, +180^\circ]$	$[0^\circ, 360^\circ]$
0	-0.00000	5.00000	-45.00000	315.00000
45	-82.94677	45.21762	40.01893	40.01893
90	-85.00000	90.00000	45.00000	45.00000
135	-82.94677	134.78238	49.98107	49.98107
180	-0.00000	175.00000	135.00000	135.00000
225	82.94677	134.78238	-139.98107	220.01893
270	85.00000	90.00000	-135.00000	225.00000
315	82.94677	45.21762	-130.01893	229.98107
360	0.00000	5.00000	-45.00000	315.00000

Table 6: Table of ψ for $\psi_{uv} = 270^\circ$ and $\psi_{uv} = 315^\circ$.